



Stockholm
University

Bachelor Thesis

Degree Project in
Geochemistry 15 hp

Exploring reverse weathering processes in Baltic Sea sediment pore waters

Johanna Waldheim



Stockholm 2018

Department of Geological Sciences
Stockholm University
SE-106 91 Stockholm
Sweden

Johanna Waldheim
Stockholm University
Institution of Geological Science

Abstract

Early diagenesis is catalysed by microbial life in marine sediment by utilising solutes to decompose organic carbon. The reactant solutes are controlled by the amount of change in free energy in the reaction. Solute are transported to the sediment by turbulent diffusion, and inside the sediment by molecular diffusion. Ecosystems inside the sediment can rearrange pore water distribution and enable molecular motion.

Reverse weathering is a diagenetic process that form authigenic aluminosilicates, while releasing carbon dioxide and water. The reaction is limited by biogenic silica and degraded clay minerals, which reacts with bicarbonate and solutes. The carbon dioxide causes acidity in the reaction zone.

This study investigates the occurrence of reverse weathering processes in Baltic Sea sediment, and explores the possibility of a rapid reaction within the sediment. Pore water was analysed using different methods to detect precipitation patterns in solutes and alkalinity in concentration profiles, at similar depths as acidity.

Results showed an overlapping consumption path between dissolved silica and iron over a depth interval. Decreasing alkalinity and pH were discovered within the consumption depth interval.

Evidence for reverse weathering have been found in sediment, but cannot be concluded as more analysis needs to be made. More diagenetic processes need to be considered regarding the acidity and alkalinity changes.

Table of contents

1.Introduction	3
1.1 Background	3
1.2 Hypothesis	5
1.3 Aim	6
1.4 Sample settings	6
2.Method	6
2.1 Sampling method	6
2.2 Extraction of pore water	8
2.2 Oxygen, temperature and salinity in water column	9
2.3 Microsensors	9
2.3.1 Oxygen	9
2.3.2 pH	10
2.4 pH and alkalinity	12
2.5 Silica	13
2.6 Iron content	14
2.7 Sample treatment	14
2.8 Modelling	14
3.Result	15
3.1 Oxygen	15
3.2 Solutes	19
3.2 pH and Alkalinity	21
3.3 Models	24
4.Discussion	26
6. Summary and outlook	30
7.Conclusion	30
8.Acknowledgment	30
9. References	30
10. Appendix	33
10.1 Oxygen calibration	33
10.2 Calibration for determination of H_2SiO_2	33
10.3 Calibration Fe^{+2}	34
10.4 pH calibration	34
10.5 Oxygen	35
10.6 pH	37
10.7 CTD	39

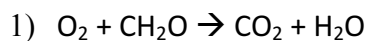
1. Introduction

1.1 Background

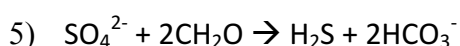
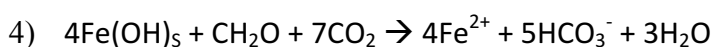
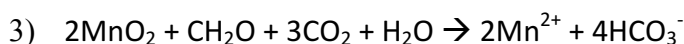
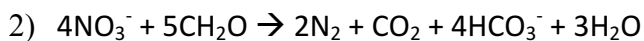
Early diagenetic processes occur in the upper millimetre in the sediment strata, after deposition. Diagenesis consists of redox reactions, catalysed by bacteria which decompose organic carbon. These affects the pH levels in the sediment, and fluxes between the water and sediment interface. Energy released by these redox reactions is used for bacteria functions, such as cell growth. The amount of energy converted by the reactions depend on the change in free energy of the reactants and their concentrations (Schoultz, 2006).

The change in free energy controls the order in which reactions occur, leading to a classical diagenetic sequence. Results from pore water analysis show patterns of precipitation and dissolution in form of concentration variations, which acts as indicators for these reactions. The main reactive oxidant for each reaction layer define the dominant degradation process (Aller, 2014), and control pH and alkalinity for specific depth.

The main oxidants in the reaction sequence is following; O_2 , NO_3^- , MnO_2 , $FeOOH$, SO_4^{2-} and CO_2 . These oxidants are involved in following exemplified reactions;



The reaction causes acidity as carbon dioxide react with water to form carbonic acid (Fossing, 2004).



The release of bicarbonate in these reactions increase the alkalinity in the pore water (Berner and Berner, 1996).

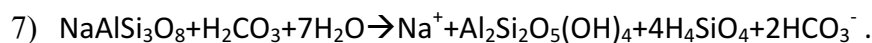
Physical and chemical properties of the above lying water column control the intensity of these reactions, along with thickness of reaction layer (Du, et al., 2018).

The movement of dissolved material from water column down to sediment pore water is dominated by turbulent diffusion. In a vertical flow direction, the turbulent diffusivity is decreasing as the sediment surface is approached. Diffusion rates is inversely proportional to distance, thus is molecular diffusion dominant in sediment. Clay minerals have a platey structure which decrease permeability properties, which enhance turbulent diffusion (Jørgensen, 1990). The diffusive boundary layer is an area right between sediment and water interface in which the turbulent diffusion is decreasing relative to molecular diffusion (Schulz, 2006). The thickness of this layer is an important factor to vertical fluxes between sediment and water accordingly to Fick's law (Jørgense, 1990);

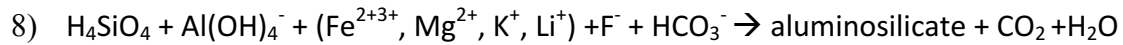
$$6) \quad J = \frac{D(C_{\infty} - C_0)}{Z_{\delta}}$$

D is the molecular diffusive coefficient for the solute of interest, C_{∞} is the bulk concentration of solute in water column, C_0 is the concentration of the solute at water and sediment interface, and Z_{δ} is the thickness of the diffusive boundary layer (Jørgensen, 1990 and Crank, 1975). In sediments with abundant macro and meiofauna, transport of pore water is also controlled by advection (Fossing et al., 2004). Bioturbation and bioirrigation contribute to displacement and mixing of pore water, which also affect distribution of solutes (Schulz, 2006).

Chemical weathering of minerals affect fluxes of solutes from terrestrial areas to marine environment. Solutes from silicate and carbonate dissolution are transported through riverine transport in to the ocean as cations (e.g. Fe^{2+3+} , Ca^{2+} , Na^+ , Mg^{2+} , K^+), silicic acid and bicarbonate. Exemplified in following weathering reaction of Albite (Berner and Berner, 1996);



Reverse weathering is a diagenetic process that form authigenic clay minerals, generally aluminosilicates, from solutes in pore water. The reaction is controlled by degraded clays and biogenic silica, which react with dissolve metal cations and bicarbonate (Aller, 2014);



Detrital material from silicates are not in equilibrium in seawater and react to achieve a stable state. The reaction may take place at the surface at a degraded aluminosilicate through adsorption-desorption or ion exchange, or between solutes. Bulk reactions of degraded clays is a slow process and does not display rapid changes in a concentration profile. Direct interactions with solutes is more rapid and show dramatic variations in concentrations (Berner and Berner, 1996).

The release of carbon dioxide balances some of the carbon dioxide extracted during chemical weathering (Mackenzie et al., 1995).

The biogenic silica in marine environments derive mainly from diatoms (Cary, 2005). Hence, the distribution of nutrients is linked to availability of dissolved biogenetic silica through diatoms (Nriagu, 1977). The terrigenous biogenetic silica constitutes for only a small fraction of the biogenetic silica dissolved in marine environments. These derive from photoliths inside vegetation (Cary, 2005).

1.2 Hypothesis

Biogenic silica should be most abundant at shallow sediment depths because of the deposition of past diatoms. As they are reactive, reverse weathering process would be most abundant at the top layer of the sediment. If the reverse weathering is the dominant process at a certain depth, concentration profiles should display a common precipitation pattern for solutes involved. The decrease in concentration could be compared with alkalinity and pH profiles which should show a decrease at the same depth. In the general reaction equation bicarbonate is extracted, which results in a decrease in alkalinity. The release of carbon dioxide and water would show a decrease in pH as carbonic acid is formed. Iron concentrations in pore water are relatively low compared to other cation concentrations. Therefore, in a concentration profile it is more sensitive to variations and enable identification of precipitation. Silica is another solute that should be analysed as it is one of the main reactants.

As many different reactions take place at the same time during early diagenesis, the process reverse weathering might not be seen in concentration profiles. Most reactions that take place to decompose carbon are releasing bicarbonate which could buffer the acidity of a simultaneous reverse weathering process. This would result in an absent offset in concentration profiles and take more detailed analysis to discover.

1.3 Aim

The aim of this project is to test the hypothesis of reverse weathering as a rapid process inside sediment in Baltic Sea.

1.4 Sample settings

Samples were collected at Fifångsdjupet, south of Trosa (**Fig.1**). Cores were taken at depths of 21 meters.

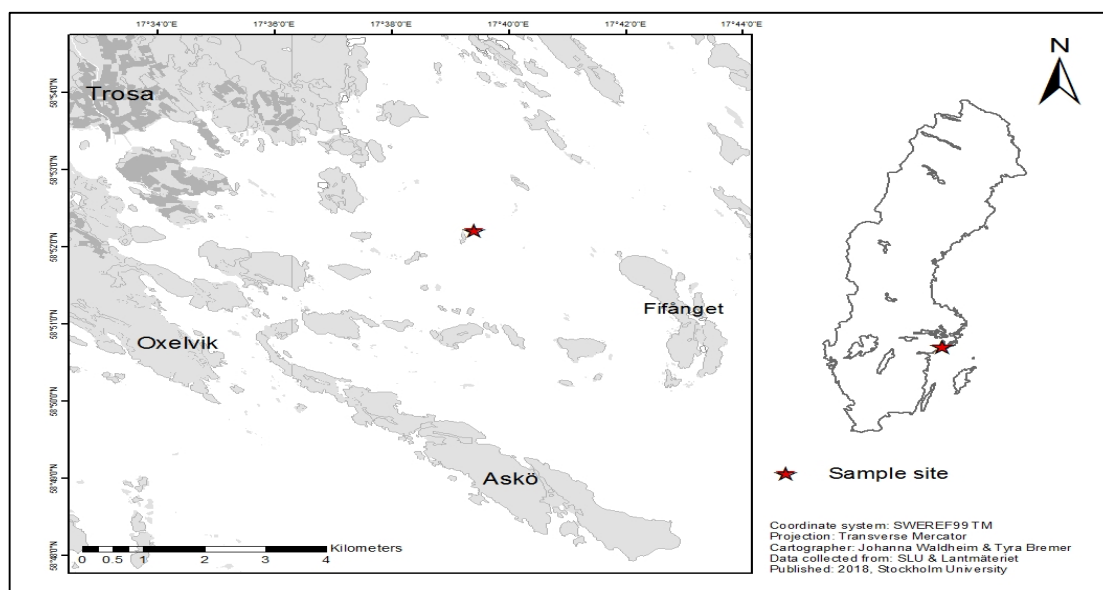


Figure 1. Map over area in which samples derived from. Red star indicates the sampling site.

2.Method

2.1 Sampling method

Sediment samples from Fifångsdjupet were taken with a multi-corer (**Fig.2**) from the research vessel Limanda. As different analyses carried out on the samples, it required that the cores were

treated differently. For sample analysis by micro-electrodes a smaller tube was inserted in the top section of the core. By adding the plug directly on the tube, a vacuum was created and it was possible to lift the smaller tube out from the bigger core. Cores taken for pore-water examination had pre-drilled holes in 10 mm intervals. The holes were covered in electric tape during this operation, to prevent sediment leakage. Water at the sediment interface (bottom water) was also collected which the sampled cores were submerged in to keep them in a natural state during analysis. This water was collected using a niskin bottle.



Figure 2. Picture showing multi-corer used during sampling.

2.2 Extraction of pore water

Extraction of pore water was done using two different methods. First the rhizon method was used to analyse the iron concentration. This method was used to avoid as much air contact possible with the sample. Before extraction of pore water proceed, each rhizons were cleansed. Unused rhizons were put in to a bath of MilliQ-water approximately two hours before use. Used rhizons were soaked for 2 hours in 10% HCl and after rinsed with MilliQ-water. Before the rhizons were inserted through the pre-drilled holes of the core, the top water of the core was removed. This was done by creating a back pressure through a hose. The rhizons inserted into the core was connected to a three way luer-type stop-cock, and was further connected to a 10 ml plastic syringe. A vacuum was created by pulling back the syringe piston allowing pore-water in to the syringe (**Fig.3**). As the syringe is filled with pore water, the stop-cock and syringes is dethatched from the rhizon. A small sampling cup was after connected to the stop-cock, the first ml of pore water extracted was wasted. Pore water that was about to be analysed was straight pipetted from the sampling cup in to cuvettes with Ferrozine (see section 2.7).

Pore water used to analyse silica concentration and pH was extracted with a centrifuge. The advantage with centrifugation instead of rhizons method is that the results have a higher resolution. Sediment was separated by depth, by pushing up sediment from a core using a stamp. The top 30 mm was cut with a metal blade in intervals of 2 mm, after which the core was cut at 10 mm intervals down to 120 mm. The sediment was put in to labelled 25 ml centrifugation tubes. The samples were centrifuged (VWR Mega Star 1.6/1.6R) at



Figure 3. Picture showing pore water extraction using the rhizon method. Sticks were added to the syringes pistons to get sucked back in to the syringes.

4500 rotations per minute for 10 min at 5°C. The sample water was extracted from the tubes using a plastic syringe and were put in to Eppendorf cups through a 0.45 µm target filter. The samples were then stored in a cold room at 3°C.

2.2 Oxygen, temperature and salinity in water column

Measurement in the water column were done by a CTD 90M from Sea & Sun Marine Tech. The instrument was equipped with a oxygen optode, conductivity meter and temperature probe.

2.3 Microsensors

2.3.1 Oxygen

Concentration determination of oxygen was done in situ using a Unisense Clark-type microsensor, with 50 µm needle. Measurement was done by 100 µm intervals between 300 µm above sediment surface, down to 600 µm.

Measurements are done as oxygen penetrates through a membrane in to the sensor. Inside the sensor oxygen reacts with an Au-anode. The reduction generates a current which is converted to a signal, and later to a concentration accordingly to the equation derived from calibration. Signals are converted using a connected Unisense Multimeter picoampere amplifier (Unisense A/S, Denmark). Measurement intervals were controlled by motorized positioning (motor MC-232) placed on a micromanipulator. The motor was controlled by a connected PC through the software SensorTrace PRO (Unisense A/S, Denmark).

The core was placed in a bath of bottom water cooled with a cooling coil connected to a Julabo cooling unit to maintain bottom water temperature of 3°C. To enable a stable diffusive boundary layer above the sediment. Surface was gently stirred by blowing air across the surface with a glass pipette (**Fig.4**).

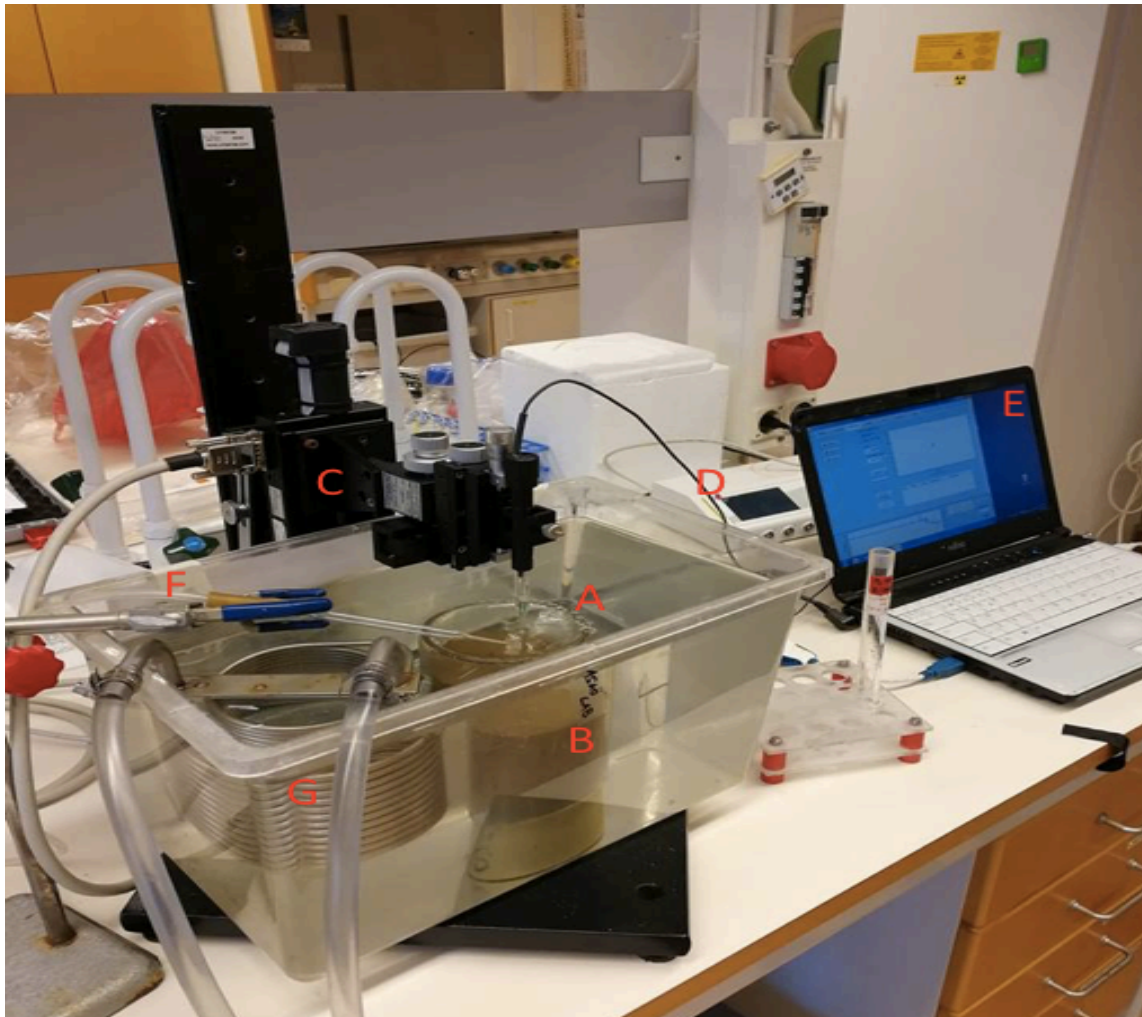


Figure 4. Picture showing set up during analysis. A) Oxygen microelectrode. B) Sample. C) Motorized system. D) Multimeter picoampere amplifier. E) PC running SensorTrace PRO. F) Glass pipette blowing air. G) Cooling Device.

Calibration of the sensor was done by equilibration in 100% saturated water and in anoxic water (Unisense A/S, Denmark). Calibrations can be found in the appendix.

2.3.2 pH

Unisense pH Microsensor together with a Unisense Reference electrode was used to determine pH. The microsensor used the same set up as during oxygen measurements (**Fig.6**). pH measurements were done with 500 μm intervals. The needle thickness was 50 μm and measurements was taken down to 4 cm depth in sediment (Unisense A/S, Denmark).

The pH electrode tip is made of glass which act as a filter. The filter is only permeable for hydrogen ions. Hydrogen iron that has penetrated the filter creates an electric potential, which

reflect the pH of the solution (Revsbech et al., 2001). The reference electrode has a Ag-AgCl electrode surrounded by an electrolyte, and is never submerged in to the sediment. It is held by a stage next to the pH sensor. The signal is read from the bottom water, and is converted to a reference signal relative to the pH sensor. The signal from the pH electrode is subtracted from reference signal, which results in a signal that represent a pH value for the measured depth (Unisense A/S, Denmark).

Calibrations (see appendix) of the sensors was made by insertion of the tips in different pH solutions, pH 4 and 7 were used.

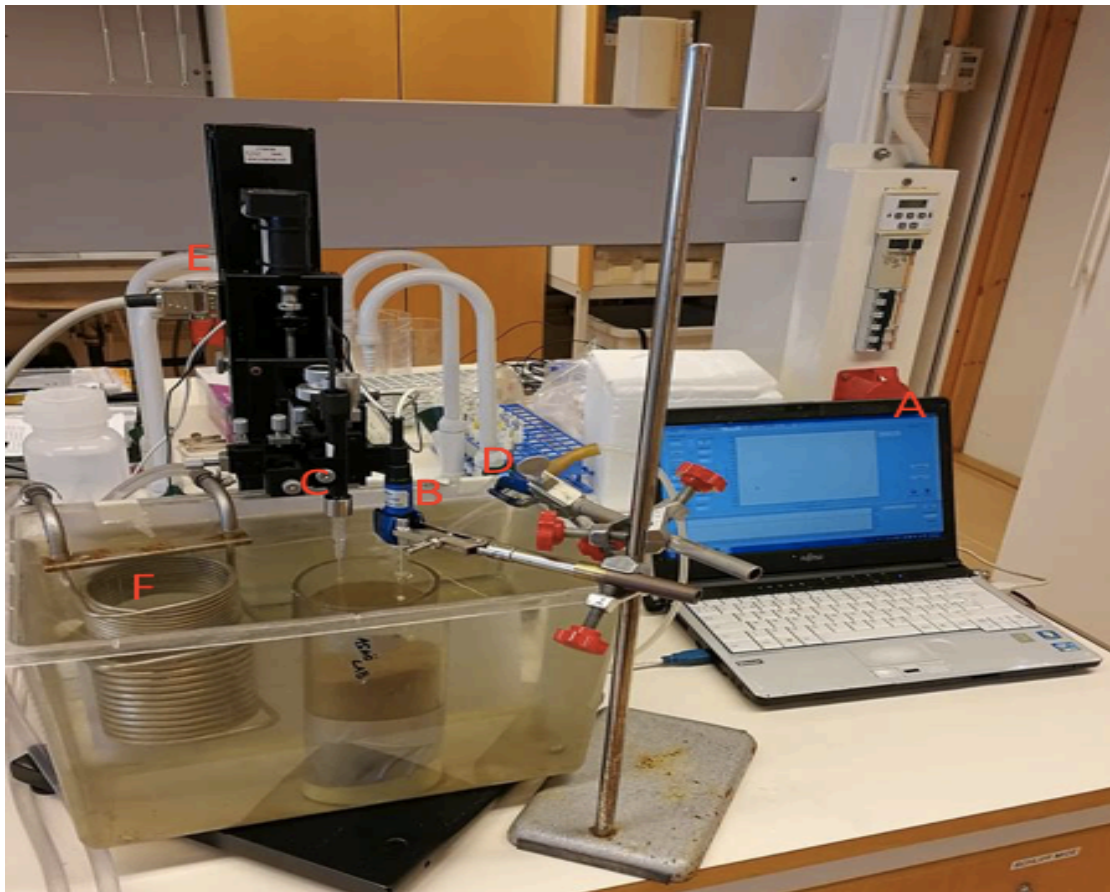


Figure 6. Picture showing set up for pH analysis. pH sensor is held with the black motorized stages, reference electrode is held by a blue clam in the stage. A) PC running Microsensor PRO. B) Reference electrode. C) pH microsensor. D) Glass pipette blowing air. E) Motorized system. F) Cooling Device.

2.4 pH and alkalinity

An automatic titration device (Metrohm Titrando 814) (**Fig.5**) was used to determine alkalinity and pH of pore water. The device was connected to a PC and calculated results using the software Tiamo. Each sample was added in to cups and weighted, after, the samples got diluted with MilliQ water to receive a volume of 25ml. The instrument measured pH using an electrode. Alkalinities were determined by adding a known volume of HCl (0.01 M) to the samples. The decrease in pH together with the added volume of acid are calculated to determine total alkalinity of the samples accordingly (Schulz et al., 2006);

$$9) \text{ Total alkalinity} = \left[(V_{HCl} * C_{HCl}) - 10^{pH} * (V_0 + V_{HCl}) * f_{H^+}^{-1} \right]$$

V_0 is the initial volume of sample, C_{HCl} is the molarity of HCl, pH is the pH value reached after HCl was added, f_{H^+} is the activity coefficient of H^+ and V_{HCl} is the volume of added acid.

The instrument was calibrated with pH 4 and 7 solutions.

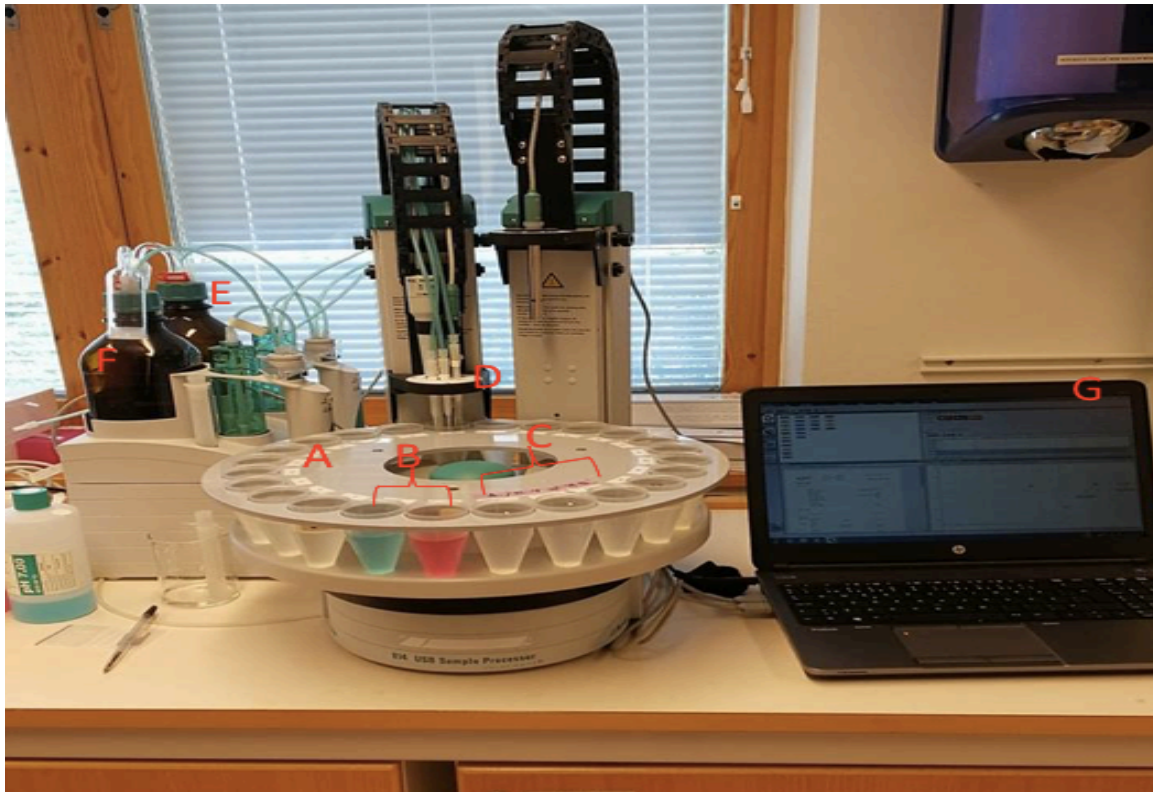


Figure 5. Picture showing the automatic titration device. A) Sample containers. B) Calibration containers with pH 4 and 7. C) Rinsing containers with MilliQ. D) Electrode, titrators and a beater. E) 0.01 M NaOH container. F) 0.01 M HCL container. G) PC running Tiamo.

2.5 Silica

A spectrophotometric method was used for determination of silica. Pore water was diluted with MilliQ water, and filled in to cuvettes (1 ml). The cuvettes were pre-filled with 0.3 ml $(\text{NH}_4)_6\text{Mo}_7\text{O}_{24}$ together with H_2SO_4 . Molybdate reacts with solutes in pore water, producing e.g. siliconmolybdate, phosphomolybdate and arsenomolybdate. Before proceeding the analysis, 10 minutes past to ensure that this reaction would be completed.

Degradation of complexes, as phosphomolybdate and arsenomolybdate, was done by adding acid. 0.2 ml ascorbic acid and 0.2 ml oxalic acid were added. The final product left in cuvettes are a blue solution consisting of siliconmolybdate.

The cuvettes were after 45 minutes inserted to a spectrophotometer (Thermo Scientific, Evolution 260 BIO), the wavelength of the emitted light was 800nm (Strickland, 1972).

Calibrations was made using the concentrations $0\mu\text{M}$, $10\mu\text{M}$, $20\mu\text{M}$, $40\mu\text{M}$ and $80\mu\text{M}$ of fused SiO_2 with NaOH (see appendix).

2.6 Iron content

The ferrozine method was used to determine iron concentration in the sediment pore water. Cuvettes were pre-filled with $50\ \mu\text{l}$ ferrozine and $500\ \mu\text{l}$ of ascorbic acid, $1\ \text{ml}$ of pore water sample were added straight after extraction from core (see section 2.2). The order in which this procedure took place was to limit air contact of the sample. To let the reaction complete, samples were left 10 minutes. Ferrozine reacts with the dissolved iron and form magenta complexes, from which absorbance is measured. The wavelength used in the spectrophotometer (Thermo Scientific, Evolution 260 BIO) during analysis was $565\ \text{nm}$.

Calibrations was done by adding $0\ \mu\text{l}$, $100\ \mu\text{l}$, $250\ \mu\text{l}$, $500\ \mu\text{l}$ and $1000\ \mu\text{l}$ of a $100\ \text{mg/l}$ stock $\text{FeSO}_4 \cdot 7\text{H}_2\text{O}$ and ascorbic acid, with $500\ \mu\text{l}$ ascorbic acid in to glass vials of $100\ \text{ml}$. MilliQ water were added to the vials to reach $100\ \text{ml}$. Ferrozine was after added together with the solution in to cuvettes (Stookey, 1970) (See calibration in appendix).

2.7 Sample treatment

Samples were kept in a freezer with a sensor controlling that the temperature stays constant at 3°C . A fan was placed inside the freezer to air the sediment cores.

2.8 Modelling

Modelling of results from concentration analysis was done with a software system called Profile. The tool generates a profile using measured profiles together with least square fits. The generated curves fit is analysed by statistical F-testing to achieve the best match with the measured profile. The gradients in generated curve is used to calculate net production and consumption, and fluxes through water sediment interface. Types of diffusion considered in the calculations are molecular diffusion and bioturbation which interact with depth and concentration accordingly;

$$10) \quad \frac{d}{dx} \left(\varphi (D_s + D_B) \frac{dC}{dx} \right) + \varphi \alpha (C_0 - C) + R = 0$$

C is the generated pore water concentration, C_0 is concentration of above lying water, depth is x, φ is porosity, D_s is the molecular diffusion coefficient (tortuosity is taken accounted for), D_B is bioturbation coefficient, α is bioirrigation coefficient and R is the net rate of consumption or production depending if the value is positive or negative (Berg et al., 1998).

3.Result

3.1 Oxygen

The results from CTD measurements (**Fig. 6**) show an increasing oxygen concentration along with water depth. Concentrations by the surface water was measured to be 379.17 $\mu\text{mol/l}$, and bottom water 408.20 $\mu\text{mol/l}$. The measured concentrations reflect well oxidised conditions in the water column. This is a result of a long winter which has decreased the water temperature, and increased solubility for gases.

Thermocline is detected right above 6 meter water depth. It is marked in the profile by rapid variations in data. The thermocline is marked as a black dotted line in the profile. The tortuosity below 6 meters is due to mixing of water with different densities.

All measurements done by the CTD can be found in appendix (See 10.7 CTD).

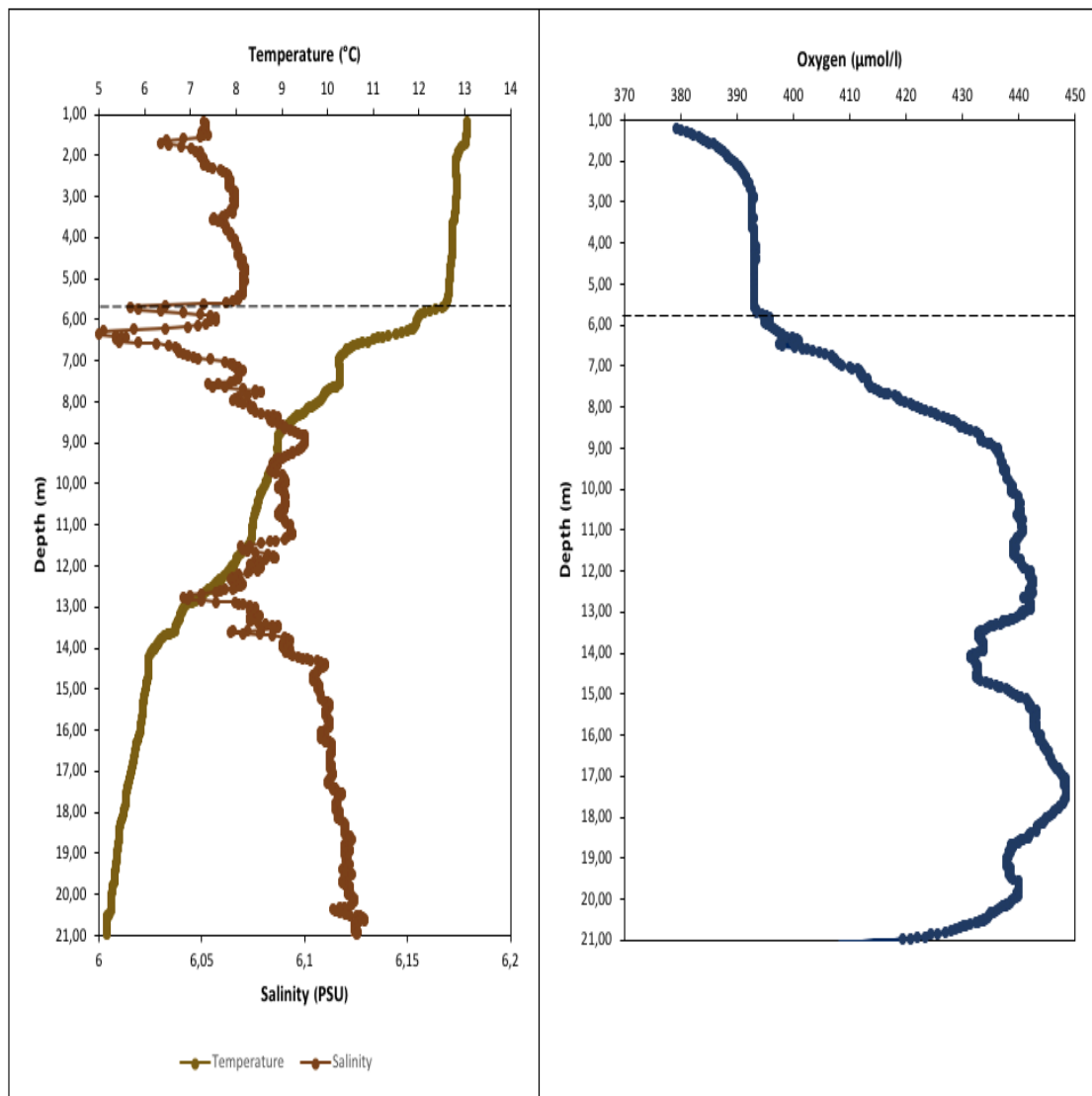


Figure 6. Profiles of temperature, salinity and oxygen. The black dotted line represent thermocline.

Results from oxygen measurements done with the microsensor (**Table 1**) show an average penetration depth approximately at 5 mm. The average thickness of the diffusive boundary layer (DBL) is 0.5 mm.

Figure 7 show a concentration profile based on one of the oxygen measurements. All measured oxygen profiles can be found in appendix (see 10.5 Oxygen). The results below the penetration depth show small variations between negative and positive values. This is due to contamination inside the sensor. Sulfide may penetrate the membrane and react which is received as a signal by the sensor.

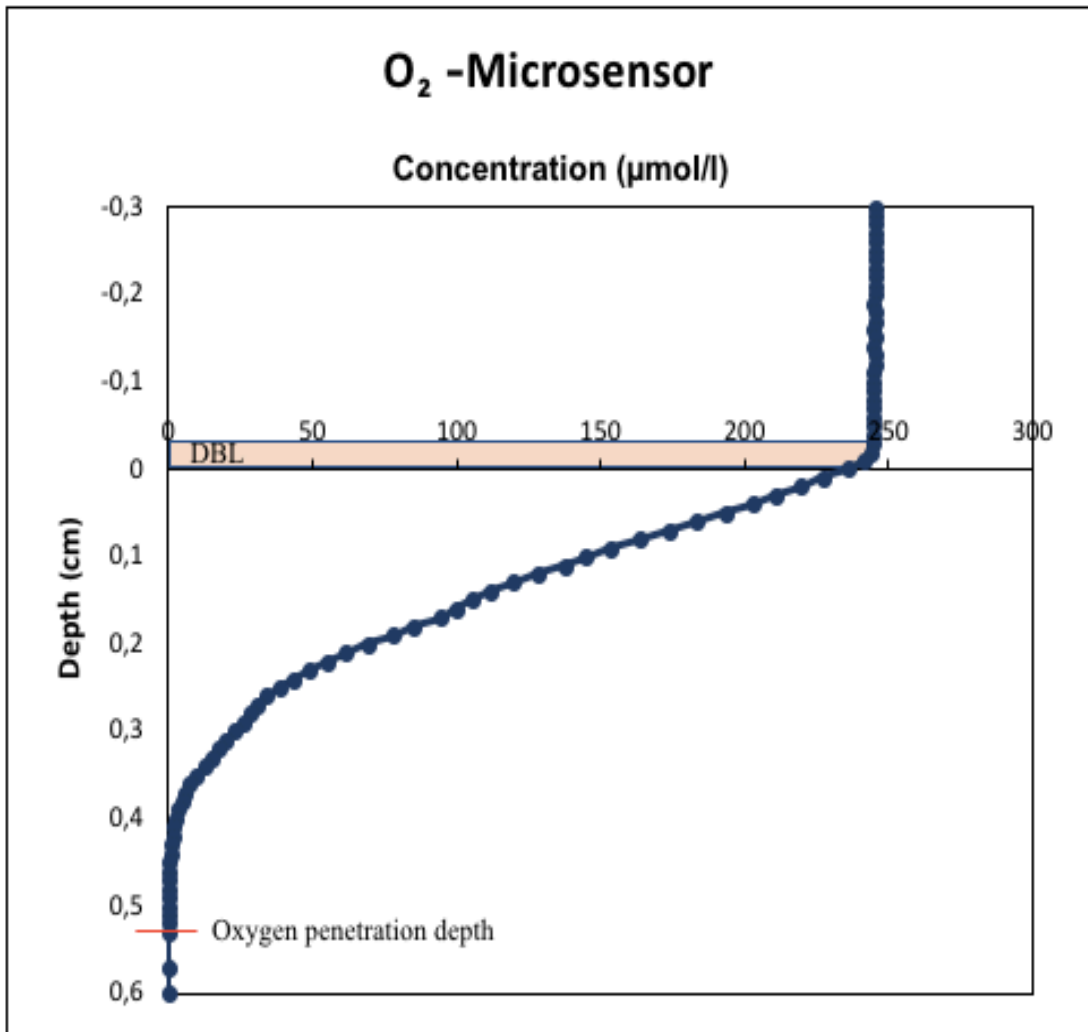


Figure 7. Concentration profile of oxygen. Pink area represents the diffusive boundary layer. Oxygen penetration depth is marked at 53 mm.

Table 1. Measured concentrations of oxygen. Negative depth values indicate measurements done above sediment surface (0 cm).

Depth (cm)	Concentration (μmol/l)	Depth (cm)	Concentration (μmol/l)	Depth (cm)	Concentration (μmol/l)
-0,3	245,21	0,05	193,16	0,4	2,44
-0,29	245,24	0,06	182,97	0,41	1,79
-0,28	245,30	0,07	174,05	0,42	1,27
-0,27	245,31	0,08	163,49	0,43	0,76
-0,26	244,94	0,09	153,52	0,44	0,40
-0,25	245,11	0,1	144,91	0,45	0,35
-0,24	245,16	0,11	137,21	0,46	0,24
-0,23	245,10	0,12	128,37	0,47	0,28
-0,22	245,11	0,13	119,66	0,48	0,22
-0,21	245,06	0,14	111,73	0,49	0,19
-0,2	245,09	0,15	105,07	0,5	0,29
-0,19	244,82	0,16	99,49	0,51	0,39
-0,18	245,09	0,17	94,52	0,52	0,26
-0,17	244,99	0,18	85,09	0,53	0,00
-0,16	244,92	0,19	78,00	0,54	-0,05
-0,15	245,07	0,2	69,04	0,55	-0,04
-0,14	244,90	0,21	61,47	0,56	-0,01
-0,13	245,04	0,22	55,42	0,57	0,03
-0,12	244,99	0,23	48,42	0,58	-0,03
-0,11	244,71	0,24	43,53	0,59	-0,09
-0,1	244,38	0,25	38,64	0,6	0,08
-0,09	244,24	0,26	33,87		
-0,08	244,48	0,27	30,90		
-0,07	244,58	0,28	28,49		
-0,06	244,81	0,29	26,03		
-0,05	244,80	0,3	23,15		
-0,04	244,78	0,31	19,91		
-0,03	244,40	0,32	17,10		
-0,02	243,48	0,33	14,69		
-0,01	241,63	0,34	12,24		
0	235,65	0,35	9,55		
0,01	227,02	0,36	7,22		
0,02	219,47	0,37	5,67		
0,03	211,07	0,38	4,50		
0,04	202,73	0,4	2,44		

3.2 Solutes

Results in analysis of dissolved silica show increase in concentration with depth. As the curve is not linear, indications of involvement in reactions are seen (**Fig. 8**).

The measured data from the analysis is presented in table 2.

Results from iron analysis (**Table 3**) display rapid increase in concentration below oxygen penetration depth (**Fig. 8**). The release of iron in pore water is due to iron reducing bacteria. Iron respiration is releasing iron cations accordingly to equation 4 (See 1.1 Background).

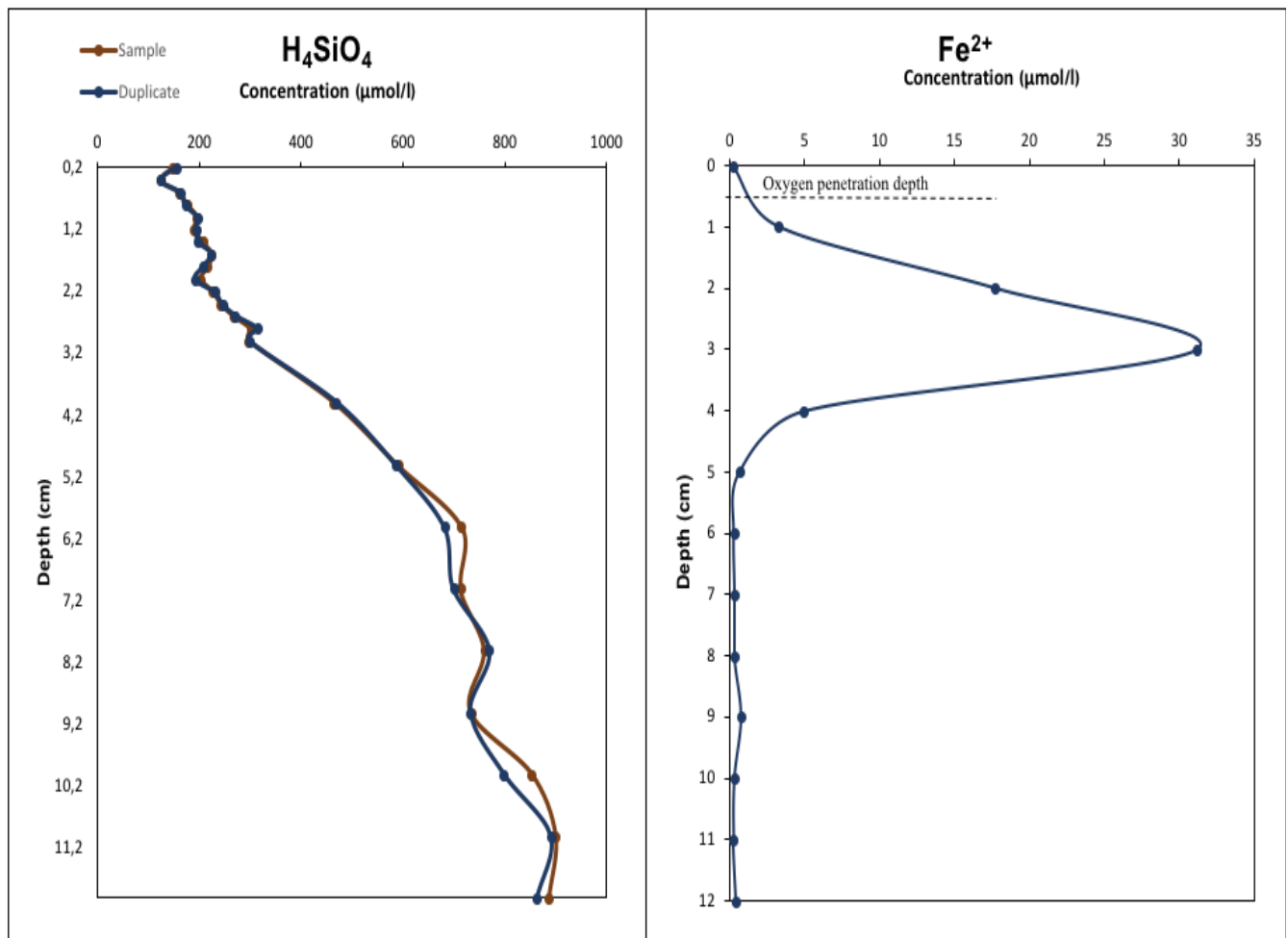


Figure 8. Concentration profiles of iron and dissolved silica.

Table 2. Results from silica analysis.

Depth (cm)	Absorbance	Absorbance	Concentration 1 (μmol/l)	Concentration 2 (μmol/l)
0,2	0,208	0,199	154,21	147,54
0,4	0,166	0,167	123,07	123,81
0,6	0,218	0,215	161,63	159,40
0,8	0,232	0,238	172,01	176,46
1	0,264	0,263	195,73	194,99
1,2	0,26	0,255	192,7	189,06
1,4	0,266	0,278	197,22	206,11
1,6	0,301	0,302	223,17	223,91
1,8	0,278	0,291	206,11	215,75
2	0,257	0,273	190,54	202,41
2,2	0,311	0,305	230,58	226,13
2,4	0,331	0,326	245,41	241,70
2,6	0,365	0,359	270,62	266,17
2,8	0,423	0,405	313,62	300,27
3	0,401	0,4	297,31	296,57
4	0,633	0,626	469,32	464,13
5	0,79	0,796	585,72	590,17
6	0,919	0,964	681,37	714,73
7	0,944	0,962	699,90	713,255
8	1,037	1,024	768,86	759,22
9	0,988	0,989	732,53	733,27
10	1,075	1,149	797,03	851,90
11	1,201	1,213	890,45	899,35
12	1,163	1,196	862,28	886,75

Table 3. Results from iron analysis.

Depth (cm)	Absorbance	Concentration (ml/l)	Concentration ($\mu\text{mol/l}$)
0	0,005	0,01	0,18
1	0,087	0,18	3,23
2	0,476	0,98	17,69
3	0,839	1,74	31,19
4	0,132	0,27	4,90
5	0,018	0,03	0,66
6	0,007	0,01	0,26
7	0,009	0,01	0,33
8	0,009	0,01	0,33
9	0,019	0,03	0,70
10	0,007	0,01	0,26
11	0,006	0,01	0,22
12	0,011	0,02	0,40

3.2 pH and Alkalinity

Results from pH measurements done with microsensor show no indications of acidity, except for one profile (see 10.6 pH in appendix). The profile data show acidity in the top 3.5 mm, below it increases pH above 7. The pH continues a relatively stable signal below 8 mm with basic conditions. The pH is decreasing after 3.8 cm and continue decreasing down to 4 cm (Fig.9). The data showed in figure 9 can be found in table 4.

Results from analysis of alkalinity and pH variations in relation to each other (Table 5). Measured values of pH does not conform with pH measured from micosensors, but follow the same general trend at some areas (**Fig. 9**). The alkalinity show a nearly linear increase in concentration below 4 cm.

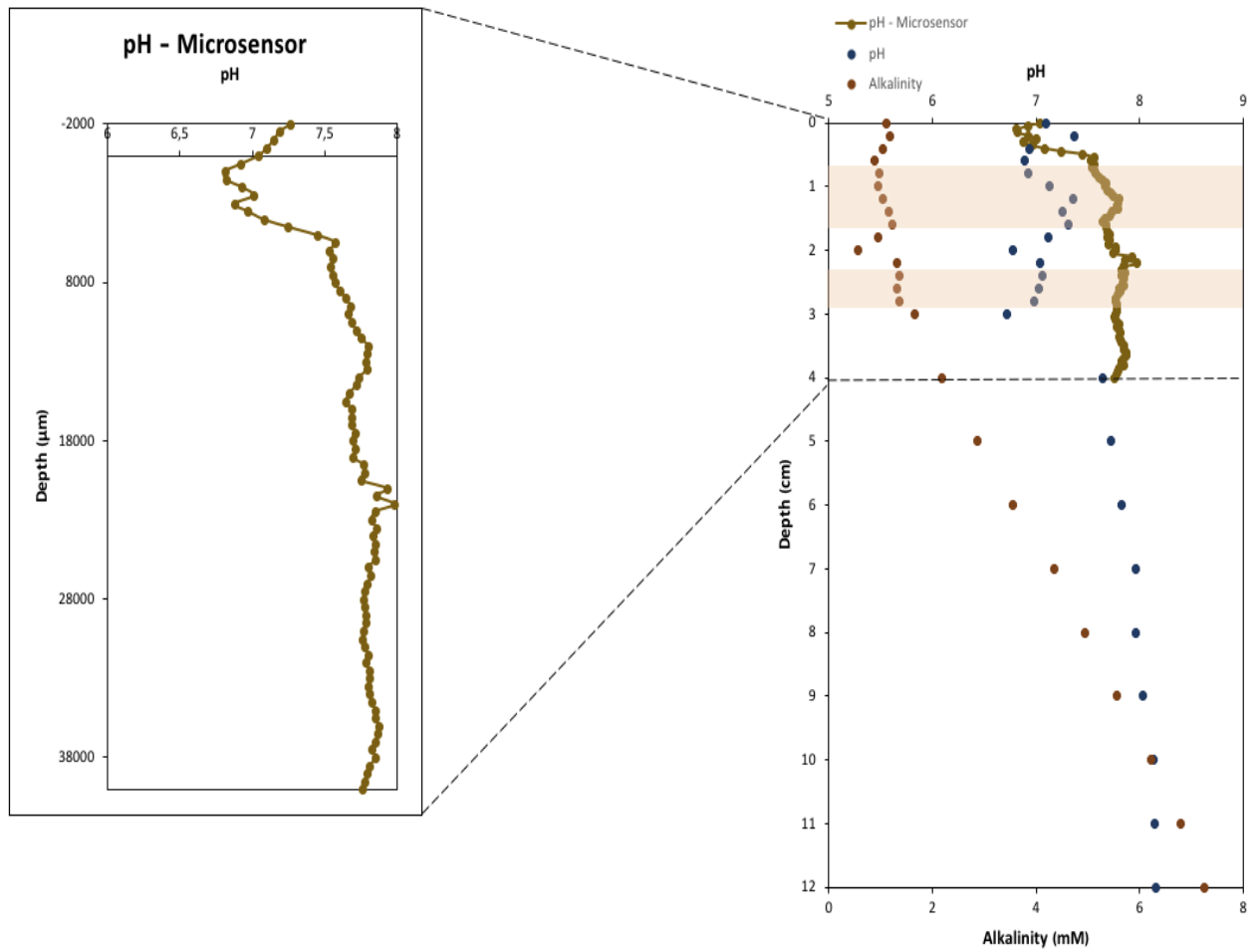


Figure 9. Plotted results of pH and alkalinity measurements. The black dotted line represents the end of microsensor measurements. The pink areas indicate areas where the data follow the same trend.

Table 4. Results from the plotted profile in figure 9.

Depth (µm)	pH	Depth (µm)	pH	Depth (µm)	pH
-2000	7,25	16 000	7,68	34 000	7,80
-1500	7,19	16 500	7,68	34 500	7,82
-1000	7,14	17 000	7,68	35 000	7,84
-500	7,09	17 500	7,70	35 500	7,85
0	7,03	18 000	7,69	36 000	7,87
500	6,92	18 500	7,71	36 500	7,86
1000	6,81	19 000	7,69	37 000	7,85
1500	6,82	19 500	7,76	37 500	7,82
2000	6,92	20 000	7,77	38 000	7,84
2500	7,00	20 500	7,74	38 500	7,80
3000	6,87	21 000	7,92	39 000	7,78
3500	6,96	21 500	7,85	39 500	7,77
4000	7,08	22 000	7,97	40 000	7,76
4500	7,24	22 500	7,85		
5000	7,45	23 000	7,82		
5500	7,56	23 500	7,85		
6000	7,52	24 000	7,82		
6500	7,55	24 500	7,84		
7000	7,53	25 000	7,84		
7500	7,55	25 500	7,85		
8000	7,57	26 000	7,80		
8500	7,60	26 500	7,81		
9000	7,64	27 000	7,79		
9500	7,678	27 500	7,77		
10 000	7,66	28 000	7,76		
10 500	7,68	28 500	7,77		
11 000	7,71	29 000	7,78		
11 500	7,74	29 500	7,78		
12 000	7,79	30 000	7,76		
12 500	7,785	30 500	7,76		
13 000	7,78	31 000	7,77		
13 500	7,79	31 500	7,80		
14 000	7,73	32 000	7,78		
14 500	7,71	32 500	7,80		
15 000	7,66	33 000	7,81		
15 500	7,64	33 500	7,79		

Table 5. Results from pH and alkalinity measurements.

Depth (cm)	pH	Alkalinity
0,2	7,37	1,17
0,4	6,93	1,04
0,6	6,89	0,87
0,8	6,92	0,97
1	7,13	0,94
1,2	7,36	1,03
1,4	7,25	1,15
1,6	7,31	1,22
1,8	7,12	0,95
2	6,78	0,55
2,2	7,04	1,30
2,4	7,06	1,35
2,6	7,03	1,31
2,8	6,98	1,35
3	6,72	1,65
4	7,64	2,18
5	7,72	2,86
6	7,83	3,55
7	7,96	4,34
8	7,96	4,94
9	8,03	5,56
10	8,13	6,22
11	8,15	6,79
12	8,16	7,24

3.3 Models

Results from flux calculations (**Table 6**) show positive flux rates for oxygen by the sediment surface, which indicate the dissolved oxygen in the water column outside the measured area. Iron has a negative value as it is in an oxidised state in the presence of oxygen. The negative value for dissolve silica is due to its accumulation pattern in sediment. Silica do not diffuse from the sediment, hence, the increased concentration along depth.

Dissolved silica is the only solute that has a positive flux value at the bottom. The value reflects the accumulation in concentration which diffuse outside the analysed area. Concentration profiles for oxygen and iron display a rapid consumption to zero or near zero, thus the negative value in flux at the bottom.

Consumption and production rates calculated for the different solutes (**Fig. 10**) display an overlapping consumption between dissolved silica and iron. Oxygen never reach a point in which the rate is 0 because of the minor errors of the electrode (See 3.1 Oxygen).

Table 6. Calculated results for the different solutes.

<u>Calculations</u>	O₂	Fe²⁺	H₄SiO₄
Concentration at top (nmol/cm ³)	2340	0.18	140
Concentration at bottom (nmol/cm ³)	0.00	0.40	880
Flux at top (nmol cm ⁻² day ⁻¹)	7160	- 35.42	-311.04
Flux at bottom (nmol cm ⁻² day ⁻¹)	-24.1	-2.51x10 ⁻⁴	35.42
Depth integrated production in each zone (nmol cm ⁻² s ⁻¹)	-718	0.00041	0.0040

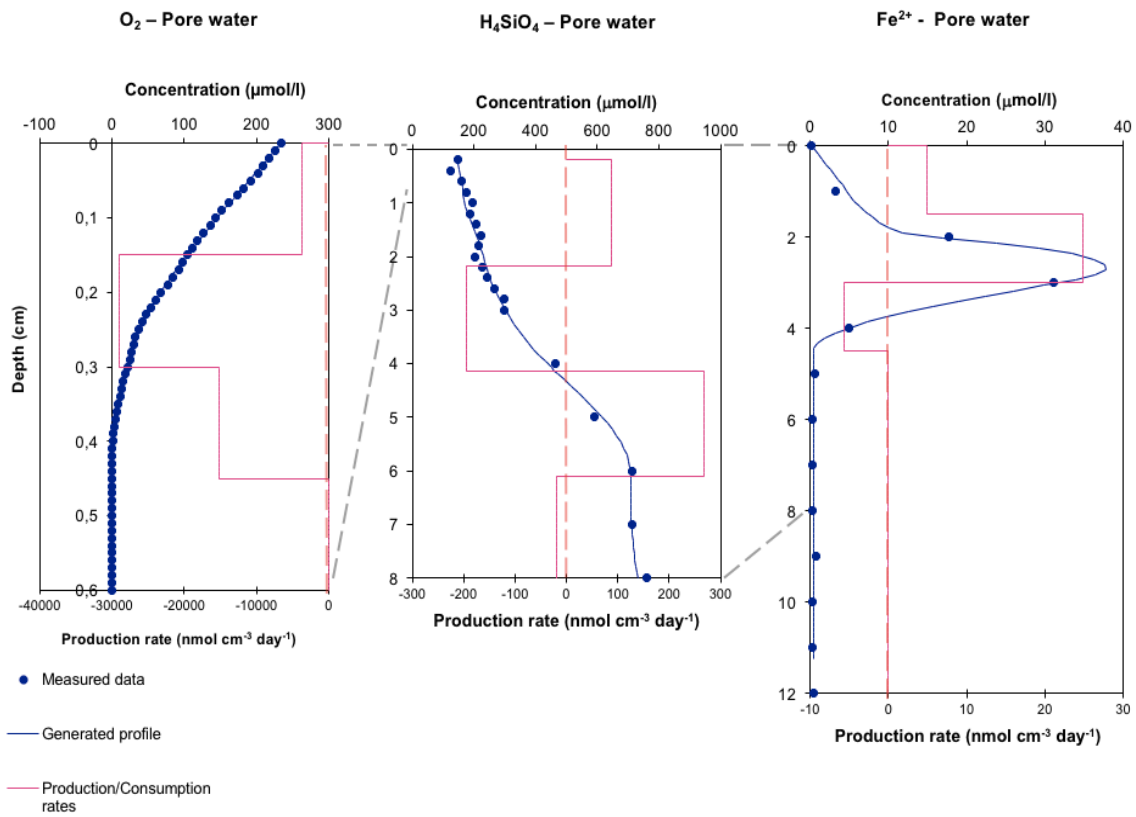


Fig.10. Plotted measurements done by modelling system. The blue dots are the measured points, the blue line is the profile generated by the software, the pink line indicate consumption/production rates.

4. Discussion

The hypothesis of reverse weathering states that acidity and loss in alkalinity should be seen in a certain area of precipitation patterns of solutes. Results from the modelling display an overlapping consumption between dissolved silica and iron, approximately between 3-4.5 cm. If the hypothesis is true, a decrease in pH and alkalinity must be seen within that interval. In data derived from the automatic titration device, there is a decrease in alkalinity and pH at 3 cm. This is not according to data from the pH microsensors, which display more general basic conditions in the sediment. Results from pH measurement are contradicting as they mostly follow different trends and direction in their data. The interpretation made by this is that there is a decrease in pH at 3 cm. As the alkalinity increases below 4 cm, the greatest probability of reverse weathering processes occurring is above 4 cm. Thus, the extraction of bicarbonate in the reaction would rather show a decrease in alkalinity (see equation 8).

The consumption of iron and the measured acidity may be explained by other processes as well. Element cycling and early diagenetic reactions occur simultaneously and effect precipitation of solutes and pH. Hence, the potential acidity may not be the result of carbonic acid.

Sulphide cycling has a great impact on acidity due to the reduction of hydrogen sulphide (H₂S).

It is possible that the pH reflects H₂S diffusing upward through anaerobic condition. As H₂O is oxidised in the presence of oxygen, it could theoretically diffuse upward to the oxygen penetration depth. Data taken from the same location by course students of Geochemical field methods (**Fig.11**) show a full consumption of H₂S at 2.5 cm (reading upward). The zone of acidity covers the reaction curve seen in the profile, along with precipitation of iron. These factors could indicate a degradation reaction of H₂S completed by iron. The reaction releases protons which produces acidity (Fossing et al., 2004);

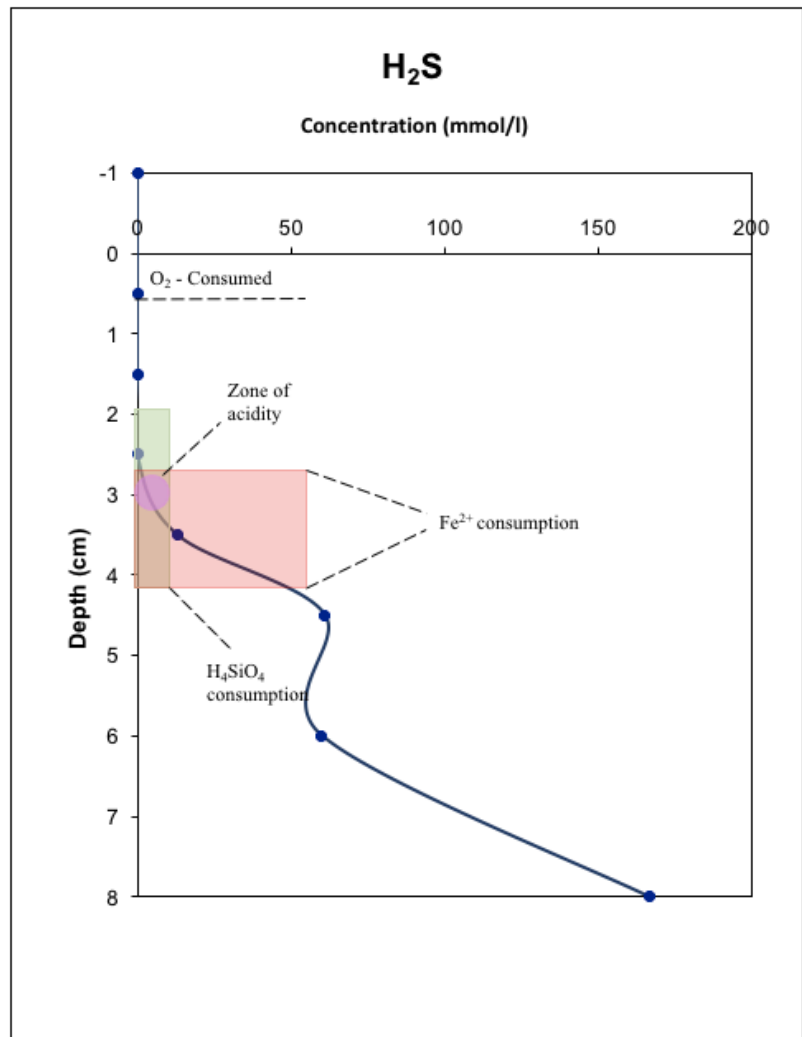
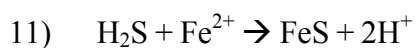
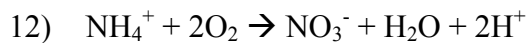


Figure 11. Concentration profile of H₂S. Pink circle represent the area of acidity, the red rectangle covers the depth of iron consumption, the green rectangle covers the depth of dissolved silica consumption.

The iron sulphide released in the process may later form pyrite in the presence of sulphur (Fossing et al., 2004).

The zone of potential acidity is too thin to explain the gradual process of H₂S reduction, and the concentration profile can display a process of H₂S production (see equation 5). Secondly, the acidity zone is too thin. Because of this, the acidity is interpreted to not be a product of H₂S.

Based on the climate for the last couple of months, denitrification is a possible explanation for the acidity. Denitrification is most intense during winter and spring (Fossing et al., 2004). The cold temperatures enable increased solubility of oxygen in water as seen in the data from CTD. The oxidised water column creates a thicker DBL as more molecular exchange occurs between sediment and water, compared to conditions during autumn. Oxygen penetration depth is also affected by temperature and is located deeper in sediment during cold conditions (Jørgensen, 1985). During nitrification oxygen degrades ammonium (Fossing et al. 2004).;



The reaction may explain the acidity measured in the top layer of the sediment, but not the acidity at 3 cm.

If the reaction of reverse weathering occurs in the sediments in Fifångsdjupet in a rapid manner, it is most probably approximately at 3 cm. This is based on the decrease of alkalinity and pH measured at that depth.

The pH measurements with microsensor did not have much variety in their values. That could indicate the possibility for a simultaneous reaction with reverse weathering, which buffer up the acidity. Hence, more alkalinity measurements should be done with higher resolution to investigate the possibility further.

The modelling of oxygen consumption rates show large values in flux at the top and bottom. The influx rate of $7160 \text{ nmol cm}^{-3} \text{ day}^{-1}$ require large amounts of organic carbon to be consumed in 5 mm depth of the sediment. The flux rates decrease as the bioturbation coefficient is set to zero (**Fig.12, Table 7**). The change in results show the importance of fauna in the aspect of transport within the sediment. The possibility of there being no fauna in oxidised sediments is very low, hence a model with no coefficient for bioturbation would not be naturally realistic. Therefore, to better estimate the oxygen fluxes, measurements in incubated sediments should be carried out. The model only present a generalised simplification of the analysed area, not results.

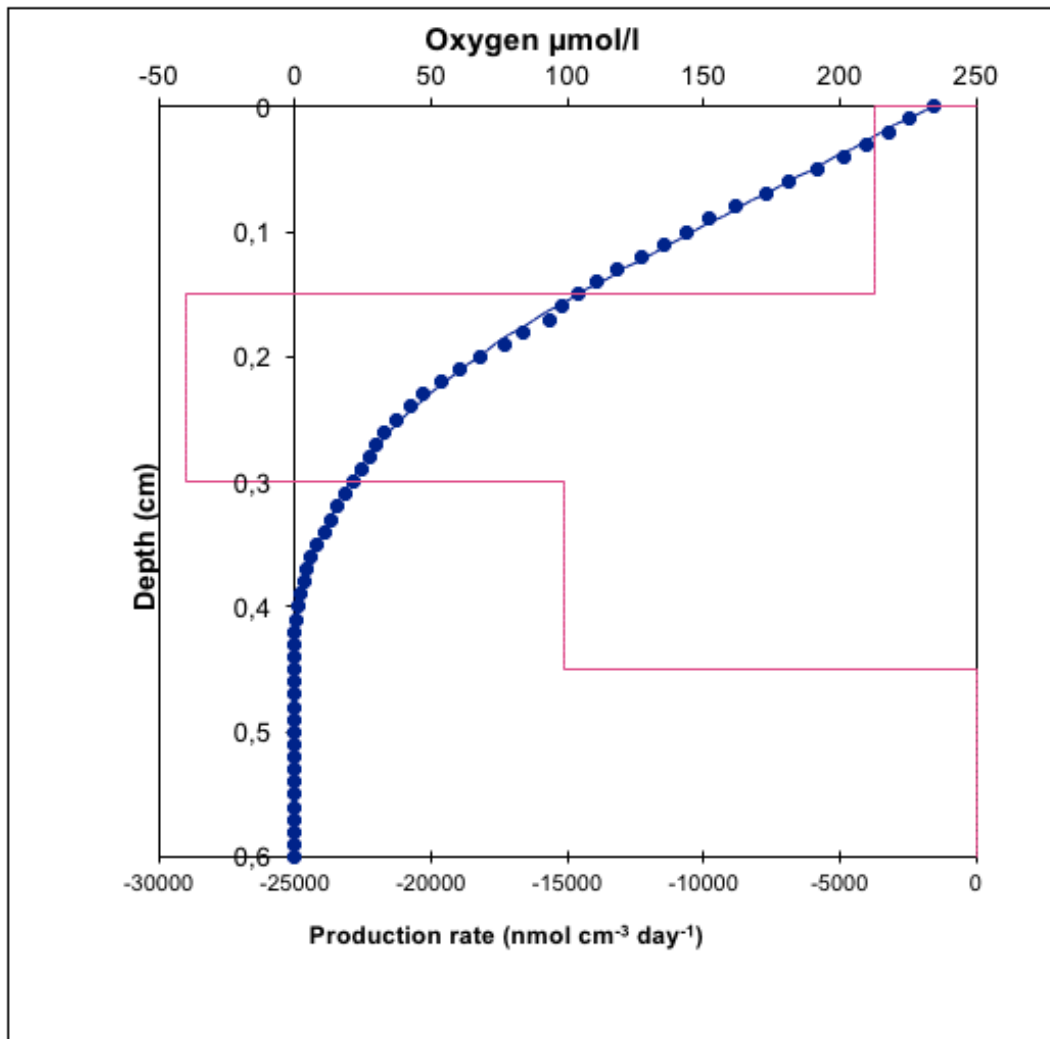


Figure 12. Plotted data from oxygen modelling without a bioturbation coefficient.

Table 7. Calculations made by modelling program without a bioturbation

Calculated concentration at top (nmol/cm ³):	235
Calculated concentration at bottom (nmol/cm ³):	0
Calculated flux at top (nmol cm ⁻² day ⁻¹):	546
Calculated flux at bottom (nmol cm ⁻² day ⁻¹):	-1.63
Depth integration of production (nmol cm ⁻² day ⁻¹):	-548

6. Summary and outlook

Based on pore water analysis, results show indications of precipitation of silica together with iron at the same depth as there is a decrease in pH. The conclusion of reverse weathering acting as the main process can be done after more detailed analysis. The results from this survey show that there are reactions occurring, but the results are too poorly detailed to determine what kind of process. To carry on this survey, one firstly needs to determine the ratios of biogenic silica and dissolved silica (Lyle et al., 2002).

As pH in sediments is strongly linked with marine element cycling, more analysis needs to be done on solutes in pore water. These results will enable elimination of potential reactions that could interfere with the solutes of interest. This could be done using different kinds of methods e.g. ion chromatography (Pfaff, 1993).

Sediment analysis is required to be done of clay minerals of the Baltic sea. That could be done using X-ray Diffraction to identify minerals, elements, element ratios and mineral structure (Moore, 1997). As carbon dioxide is released in reverse weathering processes, microsensors can be used to determine if there are increased concentrations at any certain depths.

7. Conclusion

Results showed a potential reverse weathering process at 3 cm. This was a decrease in alkalinity and pH. The decrease was in an area that had overlapping consumption rates of iron and dissolved silica. But as the results from the pH microsensor did not show any acidity at 3 cm, detailed analysis needs to be done to investigate further.

8. Acknowledgment

I would like to thank my supervisor Volker Brüchert, Wanjiao Kong for helping me during determination of silica concentration, Tyra Bremer for GIS support, and finally, Jonas Fredriksson and Malin Lindström for the help during sampling.

9. References

Aller R.C. 2014. 8.11- Sedimentary Diagenesis, Depositional Environments, and Benthic Fluxes. *Treatise on Geochemistry (Second Edition)*. Vol. 8. 293-334.

Johanna Waldheim
Stockholm University
Institution of Geological Science

Berg Peter, Risgaard-Petersen Nils, Rysgaard Søren. Interpretation of measured concentration profiles in sediment pore water. *American Society of Limnology and Oceanography* 43(7)-1500-1510.

Berner Kay Elisabeth, Berner A. Robert. 1996. *Global environment: Water, air, and Geochemical Cycles*. Prentice-hall, inc.

Cary Lise, Alexandre Anne, Meunier Jean-Dominique, Boeglin Jean-Loup, Braun Jean-Jacques. 2005. Contribution of phytoliths to the suspended load of biogenic silica in the Nyong basin rivers (Cameroon). *Biogeochemistry* 74. 101-114.

Conley J. Daniel. 2002. Terrestrial ecosystems and the global biogeochemical silica cycle. *Global Biogeochemical Cycles* 4. 16. 68-1-68-8.

Crank J. 1975. *The mathematics of diffusion – Second edition*. Oxford University press.

Fossing Henrik, Berg Peter, Thamdrup Bo, Rysgaard Søren, Sørensen Munk Helene, Nielsen Kurt. 2004. A model set-up for an oxygen and nutrient flux model for Aarhus Bay (Denmark). NERI Technical Report, No. 483.

Jørgensen Barker Bo, Marais Des J. David. 1990. The diffusive boundary layer of sediments: Oxygen microgradients over microbial mat. *The American Society of Limnology and Oceanography*, 35(6). 1343-1355.

Jørgensen Barker Bo, Revsbech Peter Niels. 1985. Diffusive boundary layers and the oxygen uptake of sediments and detritus. *The American Society of Limnology and Oceanography*. 30(1). 111-122.

Lyle W. Mitchell, Lyle Olivarez Annett. 2002. 6. Determination of biogenic Opal in pelagic marine sediments: A simple method revisited. *Proceedings of the Ocean Drilling Program, Initial reports*. 199.

Mackenzie T. Fred, Kump R. Lee. *Reverse weathering, Clay Mineral Formation, and Oceanic Element Cycles*. *Science*. Vol. 270.

Moore M. Duane, Reynolds, JR. C. Robert. 1997. *X-Ray Diffraction and the Identification and Analysis of Clay Minerals*, Second edition. Oxford University Press.

Nriagu O. Jerome. 1977. Dissolved silica in pore waters of Lakes Ontario, Erie, and Superior sediments. *Limnology and Oceanography*. 23(1).

Pfaff d. John. 1993. Determination of inorganic anions by iron chromatography. Environmental monitoring systems laboratory office of research and development U.S. Environmental protection agency Cincinnati, Ohio. 45268.

Revsbech N.P., Kühl M. 2001. *Biochemical Microsensors for Boundary Layer Studies*. B.P. Boudreau & B.B. Jørgensen (eds.). *The Benthic Boundary Layer*, Oxford University Press, New York. 180-210.

Johanna Waldheim
Stockholm University
Institution of Geological Science

Schulz D. Horst, Zabel Matthias. 2006. Marine Geochemistry – 2nd edition. Springer- Verlag Berlin. 103.

Skempton Westley Alec. 1969. The consolidation of clays by gravitational compaction. Quarterly Journal of the Geological Society. 125. 373-411.

Sommer Michael, Kaczorek Danute, Kuzyakov Yakov, Breuer Jörn. 2006. Silicon pools and fluxes in soils and landscapes-a review. J. Plant Nutr. Soil Sci. 169. 310-329.

Stookey L.L. 1970. Ferrozine – a new spectrophotometric reagent for iron. Analytical chemistry. 42. 779 -781.

Strickland J. D. H., Parsons T. R., 1972. A practical handbook of seawater analysis. Fisheries research board of Canada. 167.

Unisense A/S. 2014. Oxygen sensor user manual. January 2014.

Unisense A/S. pH and Reference electrode manual. December 2014.

Unisense A/S. 2011. Profiling system user manual. October 2011.

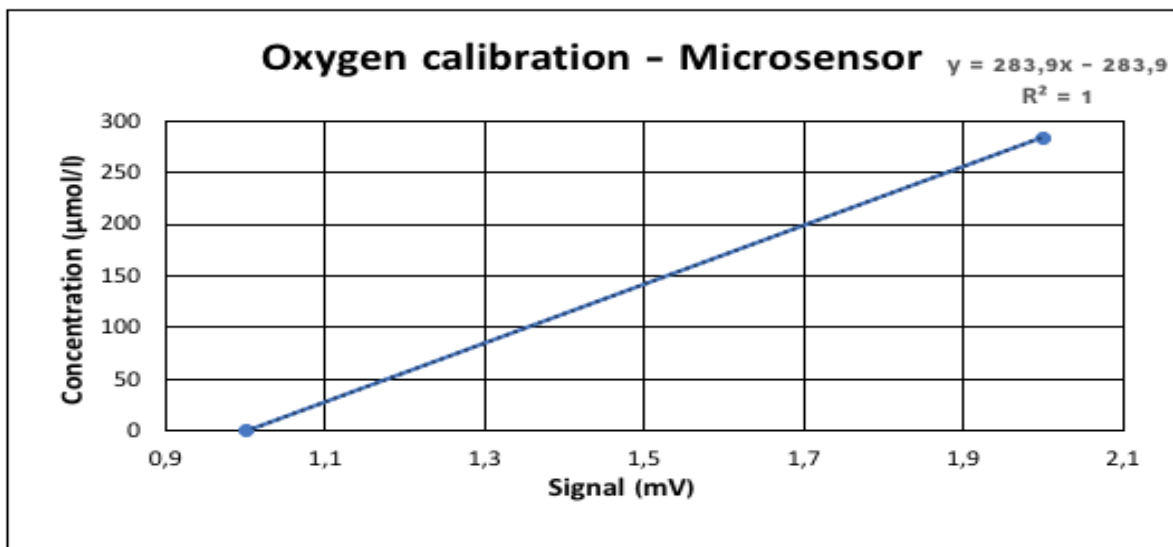
Yao Du, Teng Ma, Cong Xiao, Yanjun Liu, Liuzhu Chen, Haotian Yu. 2018. Water-rock interaction during the diagenesis of mud and its prospect in hydrogeology. International Biodeterioration & Biodegradation. 128. 141-147.

Primavera Alessandra, Trovarelli Alessandro, Andreussi Paolo, Dolcetti Giuliano. 1998. The effect of water in the low-temperature catalytic oxidation of hydrogen sulfide to sulfur over activated carbon. Applied Catalysis A: General 2. 173. 185-192.

10. Appendix

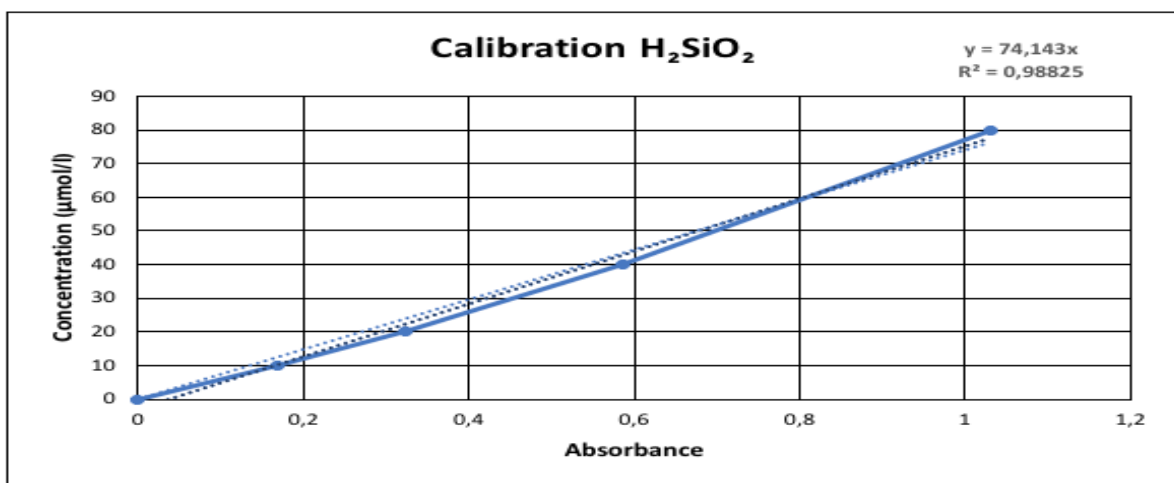
10.1 Oxygen calibration

Oxygen calibration done with the microsensor:



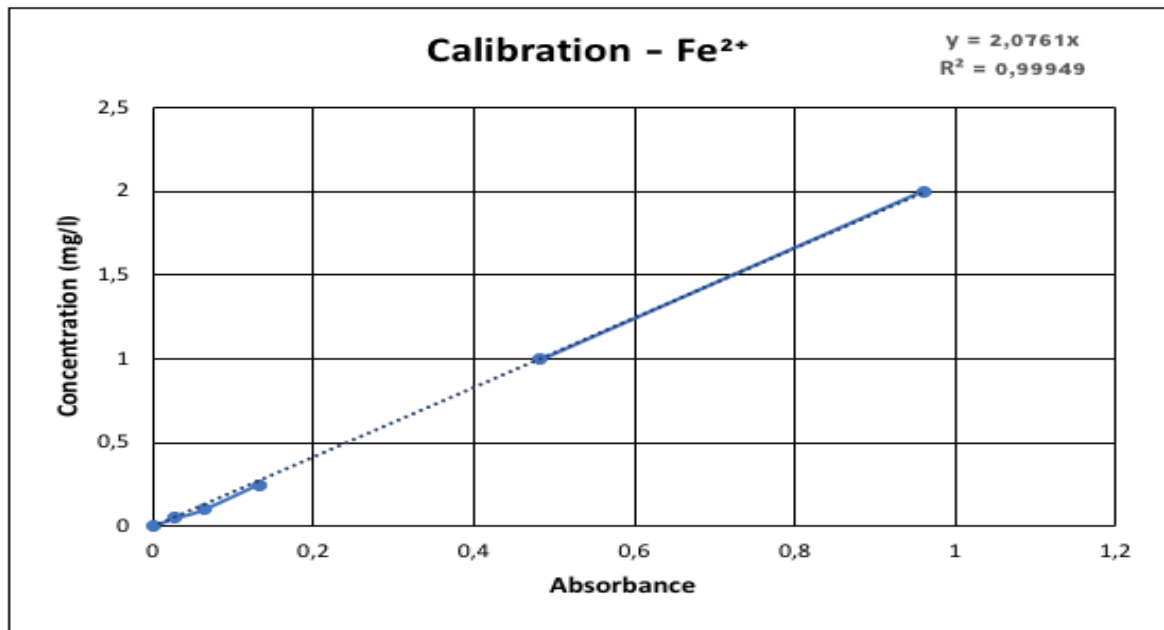
10.2 Calibration for determination of H_2SiO_2

Calibration done before analysis of dissolved silica:



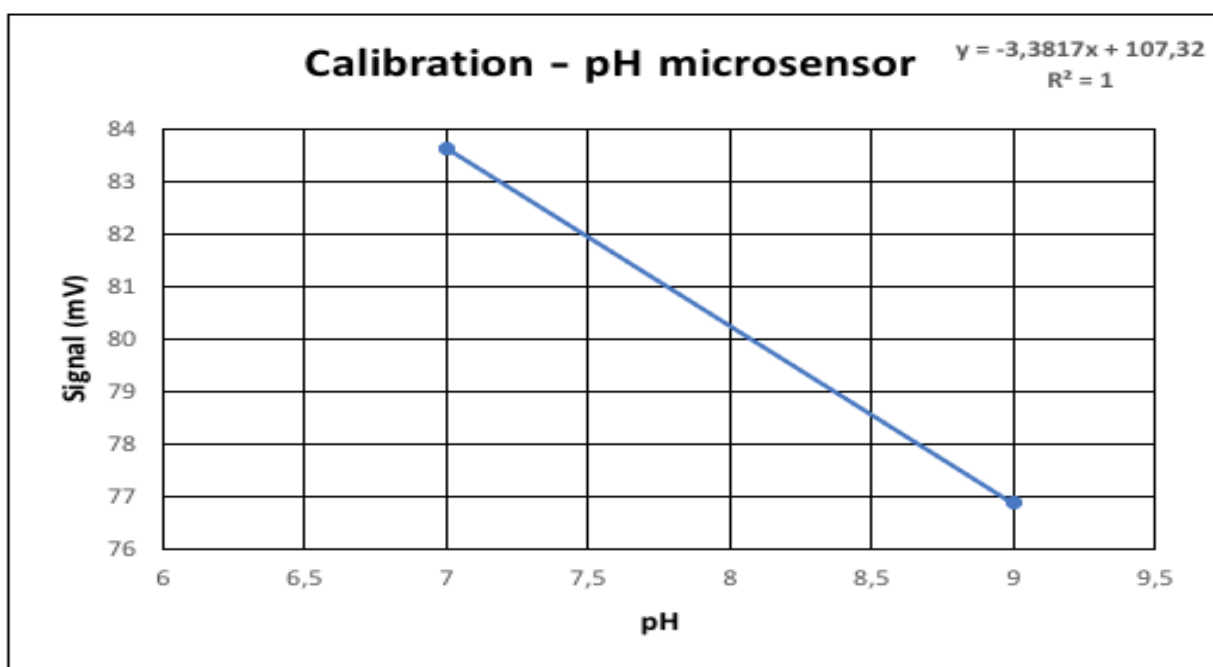
10.3 Calibration Fe²⁺

Calibration done before iron analysis:



10.4 pH calibration

pH calibration done with pH microsensor:



10.5 Oxygen

All measurements done with the oxygen microsensor:

Depth (µm)	Concentration 1 (µmol/l)	Concentration 2 (µmol/l)	Concentration 3 (µmol/l)	Concentration 4 (µmol/l)
-3000	243,07	245,21	243,22	244,83
-2900	243,13	245,24	243,52	244,81
-2800	243,26	245,30	243,63	244,88
-2700	243,14	245,31	243,73	244,60
-2600	243,12	244,94	243,80	244,56
-2500	243,16	245,11	243,89	244,95
-2400	243,02	245,16	243,99	244,91
-2300	243,06	245,10	243,95	244,70
-2200	242,83	245,11	243,93	244,74
-2100	243,00	245,06	244,23	244,83
-2000	243,13	245,09	244,15	244,95
-1900	242,90	244,82	243,89	244,71
-1800	242,85	245,09	244,12	244,56
-1700	242,91	244,99	244,01	244,72
-1600	242,80	244,92	243,93	244,79
-1500	243,13	245,07	244,03	244,66
-1400	243,10	244,90	243,87	244,62
-1300	242,95	245,04	243,74	244,75
-1200	242,93	244,99	243,50	244,77
-1100	242,64	244,71	243,21	244,72
-1000	242,58	244,38	243,08	244,85
-900	242,42	244,24	242,94	244,68
-800	242,20	244,48	242,61	244,65
-700	241,82	244,58	242,01	244,89
-600	241,41	244,81	241,09	244,91
-500	240,58	244,80	239,46	244,74
-400	239,27	244,78	237,19	244,82
-300	237,48	244,40	234,21	244,27
-200	235,92	243,48	229,52	239,54
-100	234,10	241,63	221,85	224,84
0	231,26	235,65	214,31	212,18
100	224,02	227,02	206,25	201,57
200	208,84	219,47	199,32	190,43
300	191,49	211,07	190,87	180,61
400	175,91	202,73	182,20	169,82
500	159,90	193,16	174,35	160,38
600	141,11	182,97	165,54	150,12
700	126,97	174,05	156,69	140,45
800	112,47	163,49	148,71	132,28
900	101,23	153,52	139,68	122,99
1000	90,41	144,91	131,42	115,01

1100	81,47	137,21	123,20	107,17
1200	73,24	128,37	114,59	99,02
1300	66,40	119,66	107,26	92,23
1400	58,68	111,73	99,98	85,64
1500	53,33	105,07	93,57	78,73
1600	46,53	99,49	85,66	71,94
1700	41,45	94,52	77,99	65,93
1800	36,62	85,09	70,95	59,30
1900	31,84	78,00	64,31	54,23
2000	27,81	69,04	57,69	48,03
2100	24,09	61,47	52,02	43,24
2200	19,74	55,42	45,89	38,63
2300	16,97	48,42	40,78	33,30
2400	14,08	43,53	35,11	29,36
2500	11,69	38,64	30,54	25,64
2600	8,75	33,87	26,16	21,08
2700	6,52	30,90	21,32	17,88
2800	4,98	28,49	18,08	14,76
2900	3,66	26,03	14,97	11,88
3000	2,77	23,15	12,17	8,85
3100	2,06	19,91	9,20	6,52
3200	1,56	17,10	6,65	4,61
3300	1,06	14,69	4,76	3,61
3400	0,68	12,24	3,50	2,31
3500	0,59	9,55	2,13	1,48
3600	0,52	7,22	0,94	0,85
3700	0,54	5,67	0,45	0,44
3800	0,70	4,50	0,08	0,24
3900	0,54	3,38	0,16	0,05
4000	0,56	2,44	0,01	0,14
4100	0,49	1,79	0,13	-0,07
4200	0,40	1,27	0,25	0,17
4300	0,45	0,76	0,30	-0,07
4400	0,46	0,40	0,28	-0,10
4500	0,38	0,35	0,09	-0,08
4600	0,21	0,24	0,08	0,05
4700	0,45	0,28	0,05	-0,00
4800	0,50	0,22	-0,17	0,07
4900	0,36	0,19	-0,24	0,14
5000	0,43	0,29	-0,07	-0,09
5100	0,42	0,39	-0,05	0,14
5200	0,42	0,26	0,09	-0,02
5300	0,42	0,00	-0,12	0,00
5400	0,56	-0,05	0,00	0,09
5500	0,24	-0,04	0,10	0,01
5600	0,35	-0,01	0,14	-0,10
5700	0,44	0,03	0,08	0,05

5800	0,28	-0,03	0,10	-0,04
5900	0,31	-0,09	0,09	-0,05
6000	0,22	0,08	-0,10	0,01

10.6 pH

All results from measurements done with the pH microsensor (Value with red marking is an outlier):

Depth (µm)	pH 1	pH 2	pH 3	pH 4	pH 5
-2000	7,73	8,00	7,25	7,45	7,27
-1500	7,73	7,99	7,19	7,40	7,32
-1000	7,76	7,99	7,14	7,36	7,36
-500	7,76	8,01	7,09	7,36	7,39
0	7,78	8,03	7,03	7,33	7,42
500	7,79	8,02	6,92	7,32	7,46
1000	7,80	8,03	6,81	7,32	7,48
1500	7,81	8,03	6,82	7,32	7,52
2000	7,83	8,04	6,92	7,31	7,59
2500	7,84	8,04	7,00	7,31	7,69
3000	7,85	8,04	6,87	7,33	7,75
3500	7,85	8,07	6,96	7,34	7,81
4000	7,86	8,09	7,08	7,35	7,85
4500	7,87	8,13	7,24	7,34	7,88
5000	7,89	8,16	7,45	7,35	7,93
5500	7,92	8,18	7,56	7,34	7,97
6000	7,95	8,22	7,52	7,35	8,05
6500	7,96	8,25	7,55	7,33	8,08
7000	7,94	8,26	7,53	7,33	8,11
7500	7,96	8,27	7,55	7,32	8,12
8000	7,98	8,28	7,57	7,30	8,16
8500	7,97	8,27	7,60	7,29	8,19
9000	7,98	8,30	7,64	7,27	8,24
9500	7,98	8,31	7,67	7,22	8,33
10000	7,98	8,30	7,66	7,20	8,38
10500	7,99	8,32	7,68	7,17	8,45
11000	8,02	8,31	7,71	7,14	8,47
11500	8,04	8,33	7,74	7,12	8,47
12000	8,04	8,34	7,79	7,09	8,58
12500	8,04	8,35	7,78	7,08	8,61
13000	8,07	8,35	7,78	7,06	8,60
13500	8,05	8,34	7,792	7,05	8,62
14000	8,06	8,34	7,73	7,03	8,66

14500	8,05	8,34	7,71	7,02	8,67
15000	8,08	8,34	7,66	6,99	8,74
15500	8,08	8,33	7,64	6,99	8,71
16000	8,07	8,34	7,68	6,97	8,73
16500	8,08	8,34	7,68	6,98	8,71
17000	8,06	8,32	7,68	6,97	8,74
17500	8,08	8,32	7,70	6,97	8,74
18000	8,03	8,31	7,69	6,96	8,74
18500	8,04	8,31	7,71	6,96	8,74
19000	8,03	8,29	7,69	6,96	8,73
19500	8,03	8,29	7,76	6,97	8,74
20000	8,03	8,29	7,77	6,97	8,79
20500	8,02	8,29	7,74	6,97	8,80
21000	8,01	8,29	7,92	6,99	8,83
21500	7,99	8,28	7,85	6,99	8,84
22000	7,98	8,26	7,97	6,99	8,87
22500	7,98	8,25	7,85	7,01	8,87
23000	7,98	8,24	7,82	7,02	8,86
23500	7,97	8,23	7,85	7,05	8,86
24000	7,94	8,24	7,82	7,06	8,87
24500	7,95	8,22	7,84	7,09	8,86
25000	7,94	8,22	7,84	7,10	8,84
25500	7,94	8,20	7,85	7,13	8,84
26000	7,93	8,20	7,80	7,16	8,82
26500	7,92	8,19	7,81	7,18	8,83
27000	7,93	8,18	7,79	7,19	8,76
27500	7,93	8,16	7,77	7,23	8,76
28000	7,91	8,15	7,76	7,24	8,71
28500	7,91	8,14	7,77	7,27	8,68
29000	7,92	8,13	7,78	7,29	8,64
29500	7,89	8,14	7,78	7,30	8,61
30000	7,89	8,12	7,76	7,30	8,62
30500	7,89	8,12	7,76	7,31	8,59
31000	7,87	8,10	7,77	7,32	8,55
31500	7,89	8,09	7,80	7,33	8,53
32000	7,89	8,08	7,78	7,33	8,50
32500	7,88	8,07	7,80	7,32	8,51
33000	7,88	8,08	7,81	7,35	8,50
33500	7,89	8,09	7,79	7,34	8,48
34000	7,89	8,11	7,80	7,30	8,43
34500	7,89	8,10	7,82	7,29	8,41
35000	7,89	8,10	7,84	7,29	8,38
35500	7,88	29,23	7,85	7,31	8,35
36000	7,88	8,12	7,87	7,31	8,34

36500	7,89	8,15	7,86	7,28	8,34
37000	7,88	8,14	7,85	7,28	8,35
37500	7,88	8,13	7,82	7,15	8,36
38000	7,89	8,13	7,84	7,08	8,37
38500	7,89	8,13	7,80	7,07	8,38
39000	7,90	8,13	7,78	7,07	8,39
39500	7,91	8,14	7,77	7,07	8,39
40000	7,92	8,13	7,76	7,06	8,37

10.7 CTD

All measurements done with the CTD:

Depth (m)	Temperatur (°C)	Salinity (PSU)	Oxygen (µmol/l)
1,19	13,04	6,05	379,17
1,24	13,04	6,05	380,07
1,28	13,04	6,05	380,96
1,33	13,05	6,05	381,85
1,38	13,05	6,05	382,30
1,41	13,05	6,05	383,19
1,45	13,05	6,05	383,64
1,49	13,04	6,05	384,08
1,52	13,03	6,05	384,53
1,56	13,03	6,05	384,98
1,59	13,03	6,04	385,87
1,63	13,03	6,03	386,32
1,70	13,02	6,03	386,76
1,74	12,98	6,03	387,21
1,79	12,93	6,04	387,66
1,85	12,89	6,05	388,10
1,89	12,87	6,05	388,10
1,92	12,86	6,05	388,55
1,95	12,85	6,05	388,55
1,98	12,85	6,05	389,00
2,02	12,84	6,05	389,44
2,06	12,82	6,05	389,89
2,08	12,81	6,05	389,89
2,14	12,81	6,05	390,34
2,20	12,8	6,05	390,34

2,23	12,8	6,05	390,78
2,27	12,8	6,05	390,78
2,31	12,8	6,06	391,23
2,34	12,8	6,06	391,23
2,39	12,8	6,06	391,68
2,43	12,81	6,06	391,68
2,46	12,81	6,06	391,68
2,51	12,82	6,06	391,68
2,55	12,83	6,06	392,12
2,61	12,83	6,06	392,12
2,66	12,83	6,06	392,12
2,71	12,83	6,06	392,57
2,77	12,83	6,06	392,57
2,80	12,83	6,06	392,57
2,84	12,82	6,07	392,57
2,88	12,82	6,07	393,02
2,91	12,82	6,07	393,02
2,95	12,82	6,07	392,57
3,00	12,82	6,07	392,57
3,02	12,81	6,07	392,57
3,06	12,81	6,07	392,57
3,12	12,81	6,07	392,57
3,17	12,81	6,07	392,57
3,22	12,81	6,07	392,57
3,28	12,81	6,07	392,57
3,33	12,8	6,06	392,57
3,37	12,8	6,06	393,02
3,40	12,79	6,07	392,57
3,44	12,79	6,06	392,57
3,48	12,78	6,06	392,57
3,51	12,78	6,06	392,57
3,55	12,78	6,06	392,57
3,58	12,77	6,06	392,57
3,62	12,75	6,06	392,57
3,65	12,74	6,06	393,02
3,70	12,74	6,06	393,02
3,74	12,73	6,06	393,02
3,79	12,73	6,06	393,02
3,85	12,73	6,06	393,02

3,88	12,73	6,06	393,02
3,92	12,73	6,06	393,02
3,98	12,73	6,06	393,02
4,01	12,73	6,07	393,02
4,05	12,73	6,07	393,02
4,09	12,73	6,07	393,46
4,12	12,73	6,07	393,02
4,15	12,73	6,07	393,02
4,19	12,73	6,07	393,46
4,21	12,73	6,07	393,02
4,27	12,73	6,07	393,02
4,29	12,73	6,07	393,02
4,34	12,73	6,07	393,46
4,39	12,73	6,07	393,46
4,42	12,72	6,07	393,02
4,47	12,72	6,07	393,02
4,50	12,71	6,07	393,02
4,55	12,7	6,07	393,02
4,61	12,7	6,07	393,02
4,65	12,7	6,07	393,02
4,68	12,69	6,07	393,02
4,73	12,69	6,07	393,02
4,75	12,69	6,07	393,02
4,79	12,68	6,07	393,02
4,83	12,68	6,07	393,02
4,84	12,68	6,07	393,02
4,88	12,68	6,07	393,02
4,92	12,68	6,07	393,02
4,97	12,67	6,07	393,02
4,99	12,67	6,07	393,02
5,02	12,67	6,07	393,02
5,07	12,66	6,07	393,02
5,11	12,66	6,07	393,02
5,13	12,66	6,07	393,02
5,19	12,66	6,07	393,02
5,25	12,65	6,07	393,02
5,28	12,65	6,07	393,02
5,33	12,65	6,07	393,02
5,38	12,65	6,07	393,02
5,42	12,64	6,07	393,02

5,45	12,64	6,07	393,02
5,48	12,63	6,07	393,02
5,51	12,62	6,07	393,02
5,55	12,61	6,07	393,02
5,59	12,6	6,06	393,02
5,62	12,59	6,05	393,46
5,65	12,56	6,03	393,46
5,70	12,5	6,02	393,46
5,75	12,37	6,02	394,36
5,79	12,23	6,03	395,25
5,83	12,12	6,04	395,70
5,87	12,05	6,05	395,70
5,90	12	6,05	394,80
5,94	11,98	6,06	394,80
5,97	11,96	6,06	395,25
6,01	11,95	6,06	395,70
6,05	11,94	6,05	396,14
6,09	11,93	6,05	396,59
6,14	11,92	6,05	397,04
6,17	11,89	6,04	397,48
6,22	11,87	6,03	397,93
6,24	11,82	6,02	397,93
6,28	11,75	6,00	398,82
6,32	11,63	6,00	399,72
6,35	11,49	6,00	400,61
6,40	11,33	6,01	401,06
6,43	11,21	6,01	399,72
6,45	11,1	6,01	397,48
6,49	11	6,01	397,93
6,53	10,88	6,01	400,16
6,57	10,76	6,02	401,50
6,59	10,65	6,03	402,40
6,63	10,57	6,03	403,29
6,66	10,51	6,04	404,63
6,70	10,46	6,04	405,52
6,73	10,42	6,04	406,86
6,78	10,38	6,04	406,86
6,82	10,34	6,04	407,31
6,86	10,3	6,04	407,31
6,90	10,27	6,05	407,75

6,94	10,26	6,05	408,20
6,97	10,25	6,05	408,65
7,03	10,24	6,06	409,99
7,07	10,25	6,06	410,43
7,08	10,25	6,07	411,33
7,11	10,26	6,07	411,77
7,15	10,27	6,07	411,77
7,17	10,27	6,07	411,77
7,20	10,27	6,07	412,22
7,25	10,27	6,07	412,22
7,29	10,27	6,07	412,22
7,32	10,27	6,07	413,11
7,38	10,27	6,07	413,11
7,43	10,27	6,07	413,11
7,46	10,27	6,07	413,56
7,51	10,27	6,06	413,56
7,55	10,27	6,06	414,45
7,58	10,24	6,05	414,90
7,62	10,19	6,06	415,35
7,66	10,12	6,06	416,24
7,69	10,05	6,07	416,69
7,73	10	6,08	418,03
7,75	9,96	6,08	418,47
7,78	9,94	6,08	418,47
7,80	9,93	6,08	418,47
7,84	9,92	6,07	418,92
7,89	9,9	6,07	419,81
7,93	9,88	6,07	420,71
7,95	9,85	6,07	421,15
7,99	9,8	6,07	422,05
8,03	9,74	6,07	422,49
8,07	9,69	6,07	423,39
8,12	9,64	6,07	424,28
8,14	9,6	6,08	425,17
8,18	9,56	6,07	425,62
8,24	9,51	6,08	426,51
8,27	9,45	6,08	427,41
8,31	9,39	6,08	427,85
8,34	9,34	6,09	428,30
8,37	9,3	6,09	428,75

8,41	9,26	6,09	429,19
8,47	9,23	6,08	429,64
8,50	9,19	6,08	430,09
8,54	9,15	6,09	430,53
8,58	9,11	6,09	431,43
8,61	9,08	6,09	432,32
8,64	9,04	6,09	432,77
8,69	9,01	6,09	433,21
8,73	8,98	6,10	433,21
8,78	8,95	6,10	433,21
8,81	8,94	6,10	433,21
8,83	8,92	6,10	433,66
8,87	8,91	6,10	434,55
8,90	8,91	6,10	435,00
8,95	8,91	6,10	435,44
8,99	8,91	6,10	435,89
9,02	8,91	6,10	436,34
9,05	8,91	6,10	435,89
9,09	8,91	6,10	436,34
9,13	8,91	6,10	436,34
9,15	8,9	6,10	436,34
9,19	8,91	6,10	436,78
9,22	8,91	6,09	436,78
9,26	8,91	6,09	436,78
9,29	8,91	6,09	436,78
9,32	8,9	6,09	436,78
9,36	8,89	6,09	437,23
9,39	8,88	6,09	437,23
9,44	8,86	6,09	437,23
9,48	8,84	6,08	437,23
9,51	8,83	6,09	437,23
9,55	8,81	6,09	437,68
9,59	8,79	6,09	437,68
9,63	8,78	6,09	437,68
9,65	8,77	6,08	437,68
9,69	8,75	6,08	437,68
9,74	8,72	6,09	437,68
9,77	8,71	6,09	438,12
9,79	8,7	6,09	438,12
9,85	8,69	6,09	438,57

9,90	8,68	6,09	438,57
9,93	8,66	6,09	439,02
9,96	8,65	6,09	439,02
9,99	8,64	6,09	439,02
10,03	8,63	6,09	438,57
10,05	8,62	6,09	438,57
10,09	8,6	6,09	439,02
10,13	8,58	6,09	439,46
10,17	8,56	6,09	439,91
10,21	8,55	6,09	439,91
10,24	8,53	6,09	439,91
10,28	8,52	6,09	439,91
10,32	8,51	6,09	440,36
10,38	8,5	6,09	439,91
10,42	8,5	6,09	439,91
10,44	8,48	6,09	439,91
10,49	8,47	6,09	439,91
10,52	8,46	6,09	440,36
10,54	8,46	6,09	440,36
10,59	8,45	6,09	439,91
10,63	8,44	6,09	439,46
10,64	8,43	6,09	439,91
10,69	8,42	6,09	439,91
10,72	8,41	6,09	440,36
10,76	8,4	6,09	440,80
10,80	8,39	6,09	440,36
10,85	8,38	6,09	440,36
10,89	8,37	6,09	440,36
10,95	8,36	6,09	440,80
10,99	8,36	6,09	440,80
11,01	8,36	6,09	440,80
11,05	8,35	6,09	440,80
11,08	8,35	6,09	440,36
11,12	8,35	6,09	440,36
11,15	8,35	6,09	439,91
11,18	8,35	6,09	439,91
11,21	8,34	6,09	439,46
11,25	8,34	6,09	439,46
11,28	8,34	6,09	439,46
11,32	8,34	6,09	439,02

11,35	8,33	6,09	439,02
11,38	8,33	6,09	439,02
11,41	8,32	6,08	439,02
11,44	8,3	6,08	439,46
11,50	8,28	6,07	439,02
11,53	8,24	6,07	439,02
11,59	8,2	6,07	439,02
11,64	8,16	6,07	439,46
11,67	8,12	6,08	439,46
11,70	8,08	6,08	440,36
11,75	8,04	6,09	440,36
11,78	8,02	6,09	440,36
11,81	8,01	6,09	440,36
11,85	8	6,08	440,36
11,87	7,99	6,08	440,80
11,91	7,98	6,08	440,80
11,95	7,96	6,07	441,25
11,98	7,94	6,07	441,70
12,01	7,9	6,08	442,14
12,05	7,88	6,08	441,70
12,10	7,85	6,08	441,70
12,14	7,83	6,07	442,14
12,17	7,8	6,07	442,14
12,21	7,77	6,07	442,59
12,24	7,74	6,07	442,59
12,27	7,71	6,07	442,59
12,31	7,68	6,06	442,59
12,33	7,64	6,07	442,14
12,37	7,61	6,07	442,14
12,40	7,57	6,07	442,14
12,43	7,54	6,07	441,70
12,47	7,52	6,07	441,70
12,50	7,5	6,07	442,14
12,52	7,47	6,07	442,59
12,56	7,43	6,07	442,14
12,58	7,39	6,06	441,70
12,61	7,35	6,06	441,25
12,63	7,3	6,06	440,80
12,68	7,28	6,05	441,25
12,72	7,27	6,04	441,70

12,75	7,23	6,04	442,14
12,81	7,17	6,04	441,70
12,84	7,11	6,05	441,70
12,87	7,04	6,06	441,70
12,88	6,97	6,07	442,14
12,93	6,93	6,07	442,14
12,95	6,91	6,07	441,25
12,97	6,88	6,07	440,80
13,01	6,86	6,08	440,36
13,03	6,84	6,08	440,80
13,07	6,83	6,07	440,36
13,09	6,83	6,07	439,91
13,13	6,81	6,07	439,46
13,15	6,79	6,08	439,02
13,18	6,78	6,08	438,57
13,20	6,77	6,08	438,12
13,20	6,77	6,08	437,68
13,23	6,77	6,08	437,23
13,25	6,77	6,07	437,23
13,27	6,76	6,07	436,78
13,29	6,76	6,07	435,89
13,32	6,75	6,07	435,44
13,34	6,73	6,07	435,00
13,38	6,72	6,08	434,55
13,42	6,7	6,08	434,10
13,44	6,69	6,08	433,66
13,47	6,68	6,09	433,21
13,50	6,68	6,09	432,77
13,53	6,68	6,09	432,77
13,56	6,68	6,08	432,77
13,58	6,68	6,07	432,77
13,59	6,67	6,07	432,77
13,63	6,63	6,06	432,77
13,65	6,56	6,07	433,21
13,67	6,49	6,08	433,21
13,70	6,43	6,08	433,21
13,74	6,39	6,09	433,66
13,77	6,35	6,09	433,66
13,81	6,33	6,09	433,66
13,83	6,32	6,09	433,66

13,85	6,31	6,09	433,66
13,89	6,3	6,09	433,66
13,90	6,29	6,09	433,66
13,92	6,27	6,09	433,66
13,94	6,26	6,09	433,21
13,97	6,24	6,09	432,77
14,00	6,22	6,09	432,32
14,01	6,2	6,09	431,87
14,03	6,19	6,09	431,87
14,06	6,18	6,09	431,43
14,09	6,16	6,09	431,43
14,11	6,14	6,09	431,43
14,15	6,12	6,09	431,87
14,18	6,1	6,09	431,87
14,22	6,09	6,10	432,32
14,25	6,08	6,10	432,32
14,28	6,07	6,10	432,32
14,30	6,07	6,10	432,32
14,32	6,07	6,11	432,77
14,35	6,07	6,11	432,77
14,37	6,07	6,11	432,77
14,40	6,07	6,11	432,77
14,41	6,07	6,11	432,77
14,45	6,07	6,11	432,77
14,47	6,07	6,11	432,77
14,51	6,07	6,11	432,32
14,54	6,07	6,11	432,32
14,58	6,07	6,11	432,32
14,63	6,07	6,11	432,77
14,66	6,07	6,10	433,21
14,69	6,07	6,11	434,10
14,73	6,06	6,11	435,00
14,78	6,06	6,10	435,89
14,81	6,05	6,11	436,34
14,84	6,04	6,11	436,78
14,87	6,04	6,11	437,68
14,90	6,03	6,11	438,12
14,93	6,03	6,11	438,57
14,98	6,02	6,11	439,02
15,01	6,01	6,11	439,46

15,06	6,01	6,11	439,91
15,09	6,01	6,11	440,36
15,11	6	6,11	441,25
15,16	5,99	6,11	441,25
15,21	5,99	6,11	441,70
15,23	5,98	6,11	441,70
15,26	5,97	6,11	442,14
15,30	5,97	6,11	441,70
15,33	5,96	6,11	442,14
15,36	5,96	6,11	442,14
15,37	5,96	6,11	442,14
15,40	5,96	6,11	443,04
15,44	5,96	6,11	443,04
15,47	5,96	6,11	442,59
15,50	5,96	6,11	443,04
15,53	5,95	6,11	443,04
15,56	5,95	6,11	443,04
15,60	5,95	6,11	442,59
15,64	5,95	6,11	442,59
15,67	5,94	6,11	442,59
15,72	5,94	6,11	443,04
15,75	5,94	6,11	443,04
15,77	5,93	6,11	443,04
15,79	5,93	6,11	443,04
15,81	5,93	6,11	442,59
15,85	5,92	6,11	443,04
15,89	5,92	6,11	443,04
15,91	5,92	6,11	443,04
15,94	5,91	6,11	443,04
15,98	5,91	6,11	443,93
16,02	5,91	6,11	443,93
16,05	5,9	6,11	443,93
16,08	5,89	6,11	443,48
16,12	5,88	6,11	443,48
16,14	5,87	6,11	443,93
16,19	5,86	6,11	444,38
16,25	5,85	6,11	444,38
16,27	5,84	6,11	444,38
16,29	5,83	6,11	444,82
16,31	5,82	6,11	444,82

16,34	5,81	6,11	444,82
16,37	5,81	6,11	444,82
16,39	5,81	6,11	445,27
16,42	5,8	6,11	445,27
16,44	5,8	6,11	445,27
16,48	5,79	6,11	445,27
16,51	5,79	6,11	445,27
16,54	5,78	6,11	445,72
16,58	5,78	6,11	445,72
16,61	5,78	6,11	445,72
16,65	5,77	6,11	445,72
16,67	5,77	6,11	446,16
16,73	5,76	6,11	446,16
16,76	5,75	6,11	446,61
16,79	5,74	6,11	446,61
16,83	5,74	6,11	447,06
16,84	5,73	6,11	447,06
16,89	5,73	6,11	447,06
16,93	5,72	6,11	447,50
16,97	5,71	6,11	447,50
17,00	5,71	6,11	447,95
17,02	5,7	6,11	447,95
17,06	5,69	6,11	448,40
17,10	5,68	6,11	448,40
17,14	5,68	6,11	447,95
17,18	5,67	6,11	448,40
17,22	5,66	6,11	447,95
17,26	5,65	6,11	448,40
17,30	5,64	6,11	448,40
17,36	5,63	6,11	448,40
17,39	5,62	6,11	448,40
17,42	5,61	6,12	448,40
17,46	5,61	6,11	448,40
17,49	5,61	6,12	448,40
17,52	5,6	6,12	448,40
17,55	5,6	6,12	448,40
17,59	5,6	6,12	447,95
17,63	5,6	6,12	447,95
17,65	5,6	6,12	447,95
17,69	5,6	6,12	447,50

17,74	5,59	6,12	447,06
17,78	5,59	6,12	447,06
17,82	5,58	6,12	446,61
17,86	5,57	6,12	446,16
17,89	5,56	6,12	446,16
17,93	5,55	6,12	445,72
17,98	5,54	6,12	445,27
18,01	5,53	6,12	444,82
18,04	5,53	6,12	444,82
18,09	5,52	6,12	444,38
18,12	5,52	6,12	444,38
18,15	5,51	6,12	443,93
18,18	5,5	6,12	443,48
18,22	5,48	6,12	443,04
18,26	5,47	6,12	443,04
18,28	5,46	6,12	443,04
18,33	5,46	6,12	443,04
18,37	5,45	6,12	442,14
18,40	5,45	6,12	442,14
18,44	5,45	6,12	441,70
18,49	5,45	6,12	441,70
18,50	5,45	6,12	441,25
18,54	5,44	6,12	440,80
18,56	5,43	6,12	440,36
18,59	5,43	6,12	439,91
18,61	5,43	6,12	439,91
18,62	5,43	6,12	439,46
18,66	5,43	6,12	439,02
18,68	5,43	6,12	438,57
18,71	5,43	6,12	438,57
18,76	5,42	6,12	439,02
18,80	5,42	6,12	438,57
18,83	5,42	6,12	438,12
18,86	5,42	6,12	438,12
18,88	5,41	6,12	438,12
18,88	5,41	6,12	438,57
18,91	5,41	6,12	438,12
18,94	5,4	6,12	438,12
18,96	5,4	6,12	438,12
18,98	5,4	6,12	438,12

18,99	5,4	6,12	437,68
19,03	5,39	6,12	437,68
19,08	5,39	6,12	437,68
19,11	5,38	6,12	437,68
19,15	5,38	6,12	437,68
19,18	5,38	6,12	437,68
19,20	5,38	6,12	438,12
19,24	5,37	6,12	438,57
19,25	5,37	6,12	438,12
19,28	5,36	6,12	438,57
19,31	5,36	6,12	438,12
19,35	5,36	6,12	438,12
19,38	5,36	6,12	438,12
19,41	5,36	6,12	438,57
19,43	5,35	6,12	438,57
19,47	5,35	6,12	438,57
19,52	5,34	6,12	439,02
19,54	5,35	6,12	439,91
19,57	5,35	6,12	439,91
19,60	5,35	6,12	439,91
19,63	5,35	6,12	439,91
19,65	5,34	6,12	439,91
19,69	5,33	6,12	439,91
19,72	5,33	6,12	439,91
19,76	5,31	6,12	439,91
19,79	5,3	6,12	439,91
19,80	5,3	6,12	439,91
19,84	5,29	6,12	439,46
19,89	5,29	6,12	439,46
19,92	5,29	6,12	439,91
19,95	5,29	6,12	439,46
19,98	5,28	6,12	439,02
20,01	5,28	6,12	439,02
20,03	5,28	6,12	438,57
20,06	5,28	6,12	438,57
20,12	5,27	6,12	438,12
20,12	5,27	6,12	438,12
20,13	5,27	6,12	437,68
20,14	5,27	6,12	437,68
20,15	5,27	6,12	437,23

20,17	5,28	6,12	437,23
20,18	5,28	6,12	436,78
20,23	5,27	6,12	436,34
20,27	5,27	6,12	435,89
20,31	5,27	6,12	435,44
20,33	5,27	6,12	435,00
20,37	5,27	6,11	435,00
20,41	5,26	6,12	434,55
20,44	5,24	6,12	434,55
20,47	5,23	6,12	434,10
20,49	5,22	6,12	433,66
20,52	5,21	6,12	433,66
20,52	5,19	6,13	433,21
20,53	5,18	6,13	433,21
20,56	5,18	6,13	432,77
20,58	5,17	6,13	432,32
20,60	5,17	6,13	431,43
20,63	5,17	6,13	430,53
20,66	5,17	6,13	430,09
20,69	5,17	6,13	429,64
20,73	5,17	6,12	428,75
20,76	5,17	6,12	427,85
20,81	5,17	6,12	426,96
20,84	5,17	6,13	425,62
20,87	5,17	6,12	424,28
20,91	5,16	6,13	423,39
20,93	5,16	6,13	422,05
20,96	5,16	6,13	420,71
20,97	5,16	6,13	419,37
21,00	5,16	6,13	418,03
21,02	5,16	6,13	416,24
21,03	5,16	6,12	414,45
21,04	5,16	6,13	412,22
21,04	5,16	6,12	411,33
21,04	5,16	6,12	410,43
21,04	5,16	6,12	409,54
21,04	5,16	6,13	409,09
21,04	5,16	6,13	408,65
21,05	5,16	6,13	408,20

Johanna Waldheim
Stockholm University
Institution of Geological Science